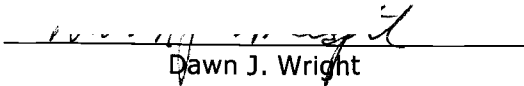


AN ABSTRACT OF THE THESIS OF

Steven C McClung for the degree of Master of Science in Geography presented on June 9, 2005. Title: Lahar Hazard Mapping of Mount Shasta, California: A GIS-based Delineation of Potential Inundation Zones in Mud and Whitney Creek Basins.

Abstract approved:

Redacted for privacy


Dawn J. Wright

Mount Shasta, the southernmost stratovolcano in the Cascade Range (41.4°N), has frequently produced lahars of various magnitudes during the last 10,000 yr. These include large flows of eruptive origin, reaching more than 40km from the summit, and studies have shown that at least 70 debris flows of noneruptive origin have occurred during the last 1,000 yr in various stream channels. The Mud and Whitney Creek drainages have historically produced more debris flows than any other glacier-headed channel on the volcano. Periods of accelerated glacial melt have produced lahars in Whitney Creek with a volume of $4 \times 10^6 \text{ m}^3$ and a runout distance of about 27 km from the summit. Mud Creek flows from 1924 – 1931 covered an area of more than 6 km^2 near the community of McCloud with an estimated $23 \times 10^6 \text{ m}^3$ of mud. A much older lahar in Big Canyon Creek may have deposited a volume of $70 \times 10^6 \text{ m}^3$ over present day Mount Shasta City and beyond. A lahar inundation modeling tool developed by USGS analysts is used to objectively delineate lahar inundation zones on Mount Shasta by embedding predictive equations in a geographic information system (GIS) that uses a digital elevation model, hypothetical lahar volumes, and geometric relationships as input. Volumes derived from these lahar deposits are extrapolated to the selected drainages to generate probable lahar inundation hazard zones with a focus on mapping and hazards implications.

© Copyright by Steven C McClung

June 9, 2005

All Rights Reserved

Lahar Hazard Mapping of Mount Shasta, California:
A GIS-based Delineation of Potential Inundation Zones
in Mud and Whitney Creek Basins

by
Steven C McClung

A THESIS
submitted to
Oregon State University

in partial fulfillment of
the requirements for the
degree of

Master of Science

Presented June 9, 2005
Commencement June 2006

Master of Science thesis of Steven C McClung presented on June 9, 2005

APPROVED:

Redacted for privacy

Major Professor representing Geography

Redacted for privacy

Chair of the Department of Geosciences

Redacted for privacy

De

I understand that my thesis will become part of the permanent collection of Oregon State University libraries. My signature below authorizes release of my thesis to any reader upon request.

Redacted for privacy

Steven C. McClung
Steven C. McClung, Author

ACKNOWLEDGEMENTS

This project would not have been possible without the help and support received from many people and organizations. I would like to thank my committee members: Dawn Wright and Jon Kimerling of the Geosciences Department at Oregon State University, and Kevin Scott of the Cascades Volcano Observatory, for their continued advice and encouragement. I would also like to thank other faculty members in the Geosciences Department for the inspiration and motivation I received from their courses: Bob Lillie, Larry Becker, Ron Doel, Julia Jones, Anita Grunder, Peter Clark, Andrew Meigs, and Anne Nolin.

I am thankful for the valuable advice given on many occasions by world-class volcanologists at the Cascades Volcano Observatory including: Dan Miller, Steve Schilling, Caroline Driedger, Jim Vallance, and Tom Pierson. I would also like to thank John Eichelberger and Pavel Izbekov from the Alaska Volcano Observatory for the awe-inspiring summer field course of 2004 in Kamchatka, which gave me a closer perspective on hazards faced by cities near active volcanoes.

I joined the Geosciences Department in 2003 with very little field experience. I want to sincerely thank the following people who got me out into the field and gave me an introduction to physical geography and geomorphology: Aaron Wolf, for a wonderful overview of Oregon's physical geography; Julia Jones and Fred Swanson, for teaching us how to ask the right questions when looking at the aftermath debris flows in the H.J. Andrews; Kevin Scott and Michelle Roberts, for time spent looking at deposits around Mount Shasta; Hugo Moreno and Claus Siebe for discussions on lahar travel and deposition over pisco sour at the foot of Osorno volcano in southern Chile. I have a great deal of appreciation for other volcanologists and students I met and learned from at the IAVCEI

general assembly in Pucon, Chile: Jean-Claude Thouret, Mike Sheridan, Lucia Capra, Gianluca Gropelli, and many others.

Special thanks to Peter VanSusteren from the USFS McCloud Ranger Station who provided me with lots of good air photos, Michelle Roberts (Humboldt State University) and Waite Osterkamp (USGS) whose work on Mount Shasta was a foundation to my thesis, and Oscar Sorenson (Michigan Tech University) who helped me in a great way in regard to LAHARZ and the DEM used.

All of this would not have been possible without the funding from the Geosciences Department teaching assistantship with Larry Becker and research assistantship with Dawn Wright. The greatest thank you goes out to my wife, Amy McClung, for her support, and to our parents for their encouragement and financial aid in the past two years. Finally and most importantly, I thank God for the grace and favor that sustains me and makes all success possible.

TABLE OF CONTENTS

	<u>Page</u>
1. INTRODUCTION	1
1.1. Background: Lahar Hazards	2
1.2. Background: Lahars Inundation Modeling	6
1.3. Research Rationale	7
2. STUDY AREA	10
2.1. Geographic/Geologic Setting and Eruptive History of Mount Shasta	11
2.2. Hydrogeomorphology	13
2.3. Site Selection	15
2.3.1 Mud Creek: Geomorphology and Debris Flow History	15
2.3.2 Whitney Creek: Geomorphology and Debris Flow History	18
2.4. Literature Review and Lahar Volume Reconstruction	22
2.4.1 Whitney Creek Lahars of 1935, 1985, and 1997	22
2.4.2 Mud Creek Lahars of 1924 – 1931	25
2.4.3 Big Canyon Creek Lahar	27
3. METHODS	31
3.1. Data collection	31
3.2. Model calibration and implementation	32
3.2.1 LAHARZ Overview	32
3.2.2 LAHARZ Implementation	34
3.2.2.1 DEM Preparation	34
3.2.2.2 Surface Hydrology Grid Generation	35
3.2.2.3 Calibration and Proximal Hazard Zone Delineation	36

TABLE OF CONTENTS (Continued)

	<u>Page</u>
3.2.2.4 Flow Volume Selection	38
4. RESULTS	39
4.1. Hazard Zones for the Whitney Creek Debris Fan	39
4.2. Hazard Zones for the Mud Creek Debris Fan	42
5. DISCUSSION	45
5.1. Digital Terrain and Model Limitations	46
5.1.1 Irregularity of Zone Boundaries	46
5.1.2 DEM Quality and Cultural Features	48
5.1.3 Other Limitations	49
5.2. Predicted Volumes and Sources of Lahars	50
5.3. Lahar Hazard Zones and Mapping Considerations	52
6. CONCLUSIONS	54
7. REFERENCES	58

LIST OF FIGURES

	<u>Page</u>
1. Eruptive Frequency of Mount Shasta, CA	2
2. Occurrence of Debris Flows on Mount Shasta Streams from 1900 to 2000	7
3. Study Area	10
4. Mud Creek Drainage	17
5. Whitney Creek Drainage	20
6. Comparison of the Extent of the 1985 and 1997 Whitney Creek Lahars	23
7. Photo of Whitney Creek tree scaring from the 1997 lahar	24
8. Photo Whitney Creek culvert at the intersection with US	25
9. The Mud Creek Debris-inundated Area From the 1924 – 1931 Lahars	27
10. Roadcut Exposure of the Big Canyon Creek Lahar	29
11. Estimate of Depositional Area for the Big Canyon Creek Lahar	30
12. LAHARZ Conceptual Diagram of Inundation Geometry	33
13. Lahar hazard zonation for the Whitney-Bolam debris fan	41
14. Overlay of 1986 Whitney Creek lahar hazard map	42
15. Lahar hazard zonation for the Mud Creek debris fan	43
16. Overlay of 1986 Mud Creek lahar hazard map	45
17. Illustration of LAHARZ methodology for cross-section construction	46
18. 3D ASTER composite showing lahar inundation area for Whitney Creek	47
19. Relationship between channel incision depth and flow frequency	51
20. Lahar warning signage at trailheads within hazard zones	53

LIST OF TABLES

	<u>Page</u>
1. Amount of debris from the 1924-1931 debris flows from Konwakiton Glacier, Mount Shasta, California	25
2. Inundation areas and runout distances for lahars in the Whitney Creek drainage	40
3. Inundation areas and runout distances for lahars in the Mud Creek drainage	44

LIST OF APPENDICES

	<u>Page</u>
Appendix A: Historic Photos of the 1924 – 1931 Mud Creek Lahars	61
Appendix B: Aerial Photography Used: Whitney Creek and Mud Creek	72
Appendix C: Previous Lahar Hazard Maps of Mount Shasta, CA.	75
Appendix D: LAHARZ Processing Sequence and Algorithm	79
Appendix E: Hazard Zonation Map for Mud and Whitney Creek Basins	81

1. INTRODUCTION

Mount Shasta is a glaciated compound stratovolcano in northern California with an eruptive frequency similar to that of Mount St. Helens, Washington (Figure 1) – about once every 800 yr (Miller, 1980). Holocene eruptive activity at Mount Shasta has produced lava flows, pyroclastic surges, tephra and hot lahars that have reached more than several tens of kilometers from the volcano. Future eruptions could endanger the communities of Weed, Mount Shasta, McCloud, and Dunsmuir, located at or near the base of Mount Shasta. Lahars (also referred to as volcanic debris flows or mud flows), are often considered the greatest hazard posed by stratovolcanoes in the Cascade Range due to their great mobility and potential to devastate valley floors tens or even hundreds of km from the source. Even during times of no eruptive activity, destructive debris flows have occurred frequently on Mount Shasta due to the existence of (1) an abundant water source in the form of seasonal snowpack, rainfall, and a glacial ice volume of approximately 140 million m³ (Driedger and Kennard, 1986); (2) steep slopes with deep failure-prone channel incisions; (3) abundant erodible and unconsolidated volcanic and glacial material.

Historic flows of eruptive and noneruptive origin at Mount Shasta have been large enough to blanket the lower flanks of the mountain with locally thick depositional terraces and alluvial fans which have now been developed and populated. Future noneruptive debris flows equal in volume to the largest historic flows could be disastrous, endangering life, property, and valuable infrastructure (Blodgett et al., 1996). At least 70 debris flows of noneruptive origin have been identified by Osterkamp et al. (1986) to have occurred within the past 1,000 yr in various stream channels. Within the past 100 yr, over 37 debris flows have occurred at an average interval of 2.3 yr between flows (Blodgett et al., 1996). Most of this activity has been focused on Mud Creek (southwest flank) and Whitney Creek

(northeast flank), which happen to be among the most deeply incised gorges on the volcano. Recent debris flows have occurred during hot summer months and have been triggered by heavy precipitation, glacier outburst floods, and floods caused by the damming of water by glacial ice or channel debris (Blodgett et al., 1996).

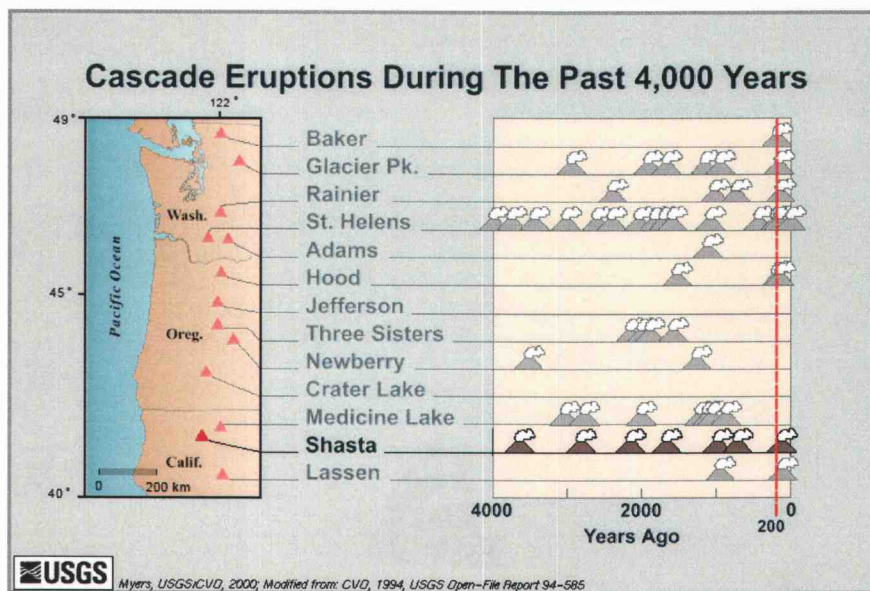


Figure 1 Eruptive frequency of Mount Shasta in relation to other Cascade volcanoes, modified from the USGS Cascades Volcano Observatory.

1.1 BACKGROUND: LAHAR HAZARDS

The 1980 eruption of Mount St. Helens removed an estimated 130 million m³ of ice and snow from the mountain, contributing to the formation of lahars and floods. Lahars that descended the southeast flank of Mount St. Helens had average flow velocities of about 67 km/hr over the 22.5 km traveled before entering a reservoir (Pierson et al., 1990). A much smaller eruption occurred in 1985 on the Nevado del Ruiz volcano in Colombia, but had the greatest impact on the built landscape. An entire village was

destroyed by catastrophic lahars, resulting in a death toll of 23,000 people. Hot pyroclastic flows interacted with snow and ice on the summit ice cap to produce large volumes of meltwater that flowed downslope, entraining loose volcanic debris to generate avalanches of saturated snow, ice, and rock. The lahar traveled up to 104 km from the source, hitting the town of Armero at 30 km/hr with a front almost 40 m high and average depth of 2 to 5 m (Pierson et al., 1990).

Lahars are gravity driven masses of water-saturated rock debris that flow rapidly downslope from a volcano. Lahars have been classified in many ways according to water-sediment concentration, rheology, and sediment characteristics (Capra et al., 2004), but most flows can be grouped into either cohesive flows, with a high clay content, or hyperconcentrated flows, which form by downstream transformation of lahars through loss of sediment and dilution by streamflow (Pierson and Scott, 1985). Additional dilution downstream may result in transformation of hyperconcentrated flows into normal streamflows, or floods.

Rock debris in lahars ranges in size from clay to blocks several tens of meters in maximum dimension. When moving, lahars resemble masses of wet concrete and tend to be channeled into stream valleys. Lahars are formed when loose masses of unconsolidated, wet debris become mobilized. Rocks within a volcano may already be saturated, or water may be supplied by rainfall, by rapid melting of snow or ice, or by a debris-dammed lake or crater lake. Lahars may be formed directly when pyroclastic flows or surges are erupted onto snow and ice, as apparently occurred in November 1985 at Nevado del Ruiz, in Colombia, where about 10 km² of snow and glacial ice were eroded to a depth of up to several m (Pierson et al., 1990). Lahars may also form as a result of debris avalanche,

flank collapse, rainfall, or glacier outburst floods. Lahar deposits may be emplaced hot or cold, depending on the temperature of the rock debris they carry.

Lahars can travel great distances down valleys, and lahar fronts can move at high speeds--as much as 100 km/hr. Lahars produced during an eruption of Cotopaxi volcano in Ecuador, in 1877, traveled more than 320 km down one valley at an average speed of 27 km/hr (Mothes et al., 1998). High-speed channelized lahars may climb valley walls on the outside of bends, and their momentum may also carry them over obstacles. Lahars confined in narrow valleys, or dammed by constrictions in valleys, can temporarily thicken and fill valleys to heights of 100 m or more (Crandell, 1971).

Lahars have occurred repeatedly during eruptions at snow-covered volcanoes in the northwestern U. S. during Holocene time. Large lahars originating in debris avalanches have occurred at Mounts Shasta, Hood, St. Helens, Rainier, and Baker, and some have been caused by the failure of debris- or moraine-dammed lakes. Small lahars are frequently generated at ice-covered volcanoes by climatic events such as heavy rainstorms and periods of rapid snowmelt due to hot weather (Miller, 1980)

In many instances, lahars have been considered to be the most serious threat to populations due to their potential speed, range, and destructive ability. This is the case for most Cascade stratovolcanoes. Even during periods of volcanic inactivity, the force of gravity on unstable, water-saturated slopes can generate destructive lahars that threaten life and property downstream. The major hazard to human life from lahars is from burial and impact by boulders and other debris. Buildings and other property in the path of a lahar can be buried, smashed, or carried away. Because of their relatively high density and viscosity, lahars can move and carry away vehicles and other large objects such as bridges. An inverse relation exists between the volume and length of lahars and their frequency,

making large lahars far less frequent than small ones. For this reason, lahar hazard progressively decreases downvalley from a volcano, and at any point along the valley, hazard from lahars decreases with increasing height above the valley floor. The largest and most frequent flows have occurred at Mt Rainier, where the volume of glacial ice is greater than that of all the other Cascade Range volcanoes combined. Geologic study of the volcano's recent eruptive history indicates that Mount Rainier has repeatedly produced lahars that would be catastrophic today due to extensive urban development in several river valleys that radiate from the volcano (Scott et al., 1995).

Mount Shasta is the most massive cone in the Cascades volcanic arc, yet it ranks last in terms of glacial ice volume¹. Despite its small glacier volume, Mount Shasta has experienced frequent climatically induced debris flows in the Holocene, triggered by warming temperatures, drought, or intense rainfall. Possibly due to its lower latitude and susceptibility to higher summer temperatures, Mt Shasta's glaciers have historically been very active. The largest of these historic lahars have been a result of climatically induced glacier outburst floods. A series of flows from 1920 to 1931 deposited roughly 5.3×10^6 m³ of mud near the historic town of McCloud, cutting off water supply, blocking roads and endangering the community. Frequent flows from Whitney Creek on the NW flank of Mount Shasta (at least nine in the past 100 yr) have destroyed parts of the Southern Pacific Railroad and Highway 97 (De la Fuente and Bachmann, 1998). Despite the sparse population in this area, summer debris flows are a persistent long term hazard. Much larger lahars from Mount Shasta associated with eruptive activity are known to have occurred before historic time. One of these flows, the Big Canyon Creek Lahar (Roberts,

¹ Seven major glaciers are recognized on Mount Shasta today, and they have a total volume of about 140 million m³ (Driedger and Kennard, 1986). This is roughly about 1/30 of the amount of ice on Mount Rainier.

2004), covers a large area on the southwestern flank of the volcano, which includes part of Mount Shasta City.

1.3 BACKGROUND: LAHAR INUNDATION MODELING

Traditional methods of delineating lahar hazard zones involve detailed study of deposit distribution, volume, and composition, as well as past flow initiation mechanisms, available historical records, and evidence of flow patterns in relation to topography. This information can be used along with calibrated flow routing models, intuition, and judgment, to extrapolate possible future inundation areas in valleys that head on volcano flank drainages.

LAHARZ, the geographic information system (GIS)-based tool used in this study, was developed by the USGS in 1998 as a method for assessing hazards from future lahars at volcanoes where data provide little basis for interpolation, extrapolation, or model calibration due to limited availability of historic and geologic records of past lahars (Schilling, 1998). Even in the case of well-studied volcanoes with a clear historic and geologic record, LAHARZ is a valuable tool for hazard zone mapping. It was not designed to comprehensively model the parameters affecting flow dynamics such as rheology, bulking rate, or superelevation. Instead, it is an automated method of delineating lahar hazard zones as a rapid, objective, and reproducible alternative to traditional, manually-plotted methods. The basic assumptions behind the methodology are similar to those of traditional methods: (Iverson et al., 1998): (1) inundation from past lahars provides a basis for predicting inundation by future lahars; (2) distal lahar hazards are confined to valleys that head on volcano flanks; (3) lahar volume largely controls the extent of inundation downstream; (4) large volume lahars are more infrequent than small lahars;

and (5) future lahar volumes are unpredictable due to the abundance of variables in their formation.

1.3 RESEARCH RATIONALE

Lahars associated with glacial outburst floods and ice avalanching have been a frequent occurrence at Mount Shasta during historic time. At least 70 debris flows have been identified by Osterkamp et al. (1986) and Hupp et al. (1987) to have occurred within the past 500 yr at Mount Shasta. The sensitivity of glaciers to pronounced warming trends has accounted for a flow frequency of about one per decade in the Mud Creek Basin and about one per 15 yr in the Whitney-Bolam drainage (Osterkamp et al., 1986), making Whitney and Mud Creek drainages the most frequently affected areas on the volcano (Figure 2).

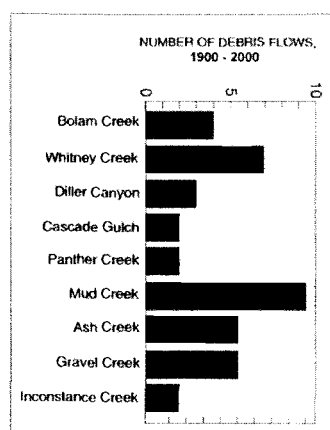


Figure 2 Occurrence of debris flows on Mount Shasta streams, 1900 – 2000. (Modified from Blodgett et al., 1996)

Some of the oldest and possibly largest lahars have occurred on the south-southwest side of the volcano, where glaciers were present in cooler times but are now absent (Roberts, 2004). Among these are several lahars identified by Dickson and Crocker (1953) which occurred during the period favoring glacial growth known as the Little Ice

Age about 100 to 300 yr ago. Short-term warming trends during episodes of glacial growth may have accounted for the formation of some of the larger lahars in Mud Creek and for the high frequency of lahar occurrence in recent centuries. Recent studies have shown that higher amounts of precipitation at Mount Shasta have resulted in the growth of its glaciers despite overall warmer temperatures (McFarling, 2003; UCSB Press Release: May 5, 2005). Therefore, it is likely that this trend of intense summer ablation during periods of increased storage may recur to some extent in the near future and again trigger series of lahars.

Lahars associated with magmatic activity on Mount Shasta are rare, but are likely to recur with the next eruptive event. Mount Shasta's last eruption occurred about 200 radiocarbon yr ago (Miller, 1980) and the geologic record suggests that it erupts at an average rate of roughly once per 250 to 300 yr (Crandell and Nichols, 1987). The known triggers of the largest possible lahars (flank collapse or debris avalanche, pyroclastic flows and surges) are all present in Mount Shasta's geologic record. With this in mind, the probability of the generation of large cohesive lahars, such as the Big Canyon Creek Lahar (Roberts, 2004) underlying Mount Shasta City, increases with time. It is therefore useful to consider probable flow paths of lahars of various magnitudes over the current topography of drainage basins. Although the focus of this study is on the two most frequent flow sites, all drainages of the volcano are susceptible to the formation of lahars and a comprehensive digital elevation model (DEM)-based lahar-inundation hazard map is needed for future hazard mitigation and continuous land-use planning.

Previous lahar-related studies of Mount Shasta have focused on characteristics of noneruptive debris flows (Osterkamp et al., 1986; Hupp et al., 1987), potential for debris avalanches (Crowley et al., 2003), flow initiation conditions (Callaghan, 2000), and the characteristics of Pleistocene and late Holocene lahar deposits on the southern flank (Roberts,

2004). Investigations of specific debris flow events at Mud Creek are included in publications by Dickson & Crocker (1953) and Hill and Egenhoff (1976). Lahar hazard maps for Mount Shasta based on field research and various dating techniques are included in publications by Miller (1980) and Osterkamp et al. (1986). The automated, GIS-based method for delineating lahar hazard zones (LAHARZ, further described in Section 4) has been used for most Cascades volcanoes as an objective way to topographically predict inundation areas. LAHARZ was designed to enhance the topographic accuracy of lahar hazard mapping and to facilitate the modeling of a variety of potential lahar volumes showing more detailed hazard gradations.

This study does not seek to produce a comprehensive lahar inundation hazard map, as an updated general volcano hazards map for Mount Shasta is currently being developed by the USGS. Instead, priority in this study is given to the two drainages of Mount Shasta most frequently affected by lahars and the issues behind the task of modeling future flow scenarios based on the empirical relationships between volume, slope and inundation area modeled by LAHARZ over digital topography. An important aspect of this work is the cartographic representation of lahar inundation hazard zones for selected watersheds.

The main research questions that stem from this objective are:

- 1) Given the known magnitude, frequency, and triggering mechanisms of past lahars, what flow volumes are possible for lahars of eruptive and noneruptive origin in the Whitney/Bolam and Mud Creek basins?
- 2) Based on local topography and debris flow modeling, what are the likely flow paths and behavior of future lahars in depositional areas?
- 3) How can a gradation of lahar hazard zones be best communicated cartographically?

2. STUDY AREA

Mount Shasta is located near the southern end of the Cascades Volcanic Arc, 65 km (40 mi) south of the Oregon border (Figure 3). It is the largest stratovolcano in the Cascade range, having produced the largest volume of eruptive products, and is the second highest, rising to 4317 m (after Mount Rainier at 4395 m).

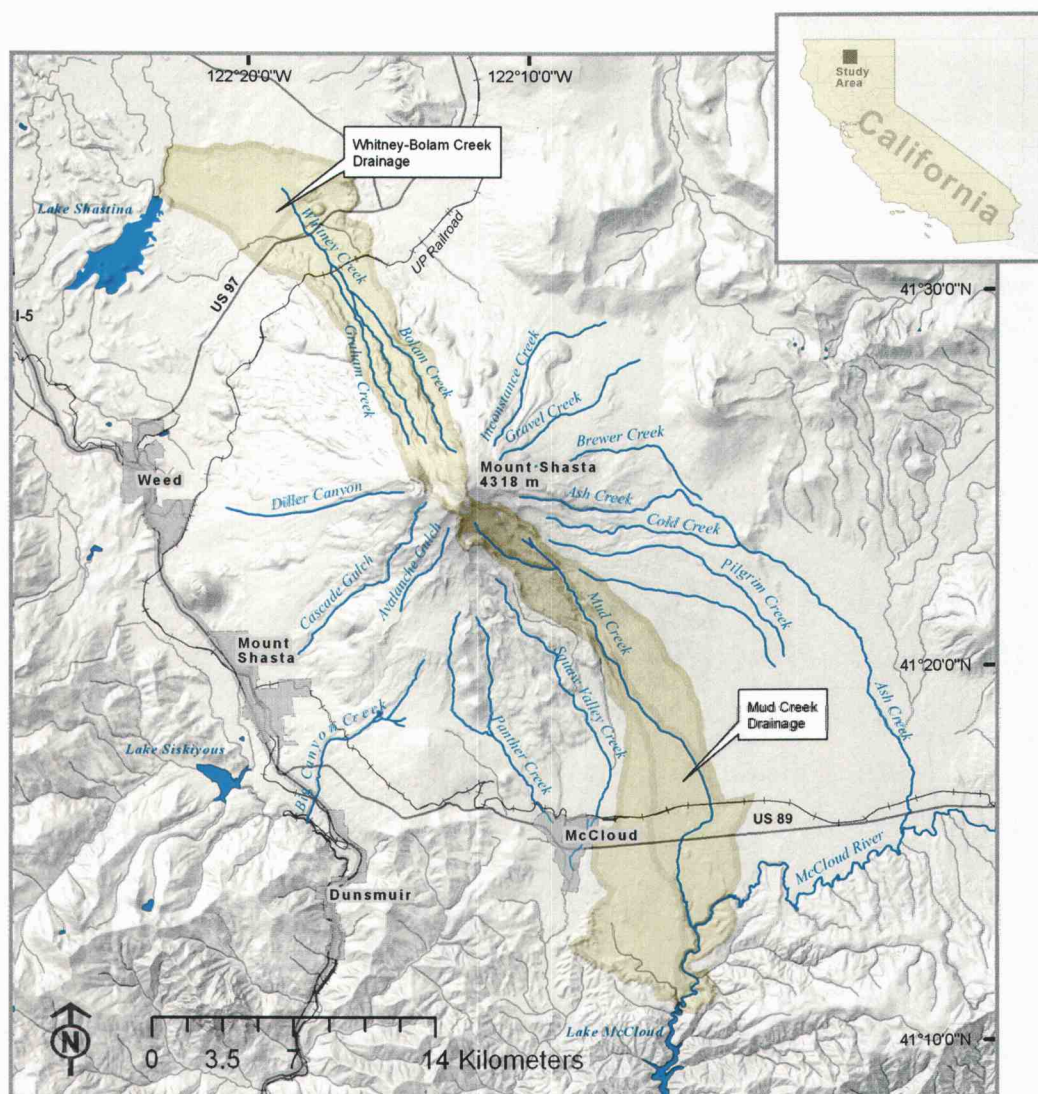


Figure 3. Map of the two study areas on the flanks of Mount Shasta bounded by the watersheds that make up the Whitney and Mud Creek basins. Towns, roads, railroads, and major streams are also shown for reference.

Mount Shasta is formed mostly of basaltic andesite and basalt flows covered by fans of unconsolidated pyroclastic, debris flow, fluvial, and glacio-fluvial deposits (De la Fuente and Bachman, 1999). The extensive occurrence of locally thick (up to 250 m) interbedded pyroclastic and debris-flow deposits on the slopes of Mount Shasta indicate that debris flows have been an important geomorphic process throughout the constructional and destructional history of the mountain (Osterkamp et al., 1986).

2.1 GEOGRAPHIC/GEOLOGIC SETTING AND ERUPTIVE HISTORY

Although Mount Shasta is relatively young, as indicated by its relatively undissected conical summit, it has been built on top of older basalts and andesites forming a number of shield volcanoes such as Everitt Hill and Ash Creek Butte, located south and east of the mountain. An outcrop of andesites on Mount Shasta's southwestern flank are the remnants of an earlier stratocone that stood on the site of the present mountain until about 350,000 yr ago (Hirt, 2004). The youngest rocks from "ancestral Mount Shasta" yielded Potassium-Argon dates of about 360,000 yr (Hirt, 2004) and were found as blocks in the massive debris avalanche that covers the western Shasta Valley with 26 km³ of material up to 43 km away from the base of the volcano.

Modern Mount Shasta has grown from the remains of its collapsed predecessor to form a composite structure of at least four overlapping cones of different ages that have produced lava flows, pyroclastic flows and domes since Pleistocene time (Christiansen, 1977 cited by Roberts, 2004, p 17). The two oldest cones, Sargents Ridge (dated at less than 250ka) and Misery Hill (dated at less than 130ka) have been deeply incised by episodes of glacial erosion. Much of today's edifice is part of the Misery Hill cone structure, which is thought to have formed sometime between 40,000 and 100,000 yr ago

(Christiansen, 2001 cited by Roberts, 2004, p 17), before the late Pleistocene glaciation. Eruptive activity continued sporadically during the glaciation, ending with the eruption of the 9,600 to 9,700- year old "Red Banks Pumice": a 350 square km pyroclastic deposit on the eastern side of the mountain (Hirt, 2004).

In contrast to the eroded pre-glacial cones, the younger Shastina and Hotlum cones were built up entirely during early Holocene time. Shastina forms a separate peak 3 km west of Mount Shasta's summit. The development of Shastina's main cone was followed by the growth of four or five small domes on the floor of its central crater. The emplacement or destruction of these dacite domes about 9500 ^{14}C yr ago (Miller, 1980), caused the western side of the cone to collapse, forming Diller Canyon and spawning pyroclastic flows that buried the present day sites of Weed and Mount Shasta City. Black Butte, another complex of dacite domes that stands next to Interstate 5 between Mount Shasta City and Weed, formed during a late phase of the Shastina episode (Hirt, 2004). Shortly after the Shastina collapse, similar events at Black Butte produced block-and-ash flows that spread about 10 km south, past the present site of Mount Shasta City, and about 5 km north to the edge of Weed (Miller, 1980).

Since the retreat of large glaciers from the mountain about 6,000 yr ago (Miller, 1980), eruptive products that formed Hotlum cone have been deposited mostly on the northeastern side of the mountain, and the dome that fills its crater forms the present summit. Early eruptions from Hotlum produced several andesitic lava flows on the northern and eastern sides of the peak, including the prominent 9-km long Military Pass flow (Hirt, 2004). Perhaps no more than 200 yr ago, explosions associated with the growth of the summit dome spread grey lithic tephra widely across the northern flank of Mount Shasta.

This most recent minor eruption in 1786 also sent a pyroclastic flow and a series of hot and cold mudflows down Ash Creek (Miller, 1980).

During the Holocene Mount Shasta has erupted approximately every 600 yr (Figure 1), with the last eruption occurring in 1786 (Miller, 1980). This eruptive frequency has made Mount Shasta one of the more active Cascade volcanoes. Currently, the main signs of thermal activity on Mount Shasta are limited to a field of sulfuric fumaroles high on the Hotlum-Bolam ridge and a small group of boiling springs just west of the summit (Hirt, 2004). The greatest noneruptive hazards posed by Mount Shasta today are from debris avalanches of hydrothermally weakened rock, and from lahars associated with frequent glacial outburst floods.

2.2 HYDROGEOMORPHOLOGY

The major drainages on Mount Shasta have all been shaped by both hot and cold debris flows carving out deep canyons from fans of unconsolidated pyroclastic, glacial, and fluvial deposits. Twelve main drainages radiate from the summit of Mount Shasta. Seven of them are headed by alpine glaciers and therefore, have had the largest and most frequent debris flow activity: Whitney, Bolam, Ash, Mud, Cold, Gravel, and Inconstance Creeks (Hupp, 1987).

Mount Shasta is surrounded by broad fans which begin relatively short distances away from the channel sources. In contrast, most other Cascade volcanoes such as Mount Rainier, Washington, are surrounded by deep stream valleys which can transport debris for long distances. Many Holocene flows of eruptive and noneruptive origin on Mount Shasta have developed these terraces and fans at relatively short distances away from the summit (Hupp, 1987). The deeply incised stream channels on Mount Shasta are generally confined

to the upper slopes above 1600m where numerous and frequent flows have deposited debris that will eventually be transported by large lahars onto the distal fan surfaces.

The areas around Mount Shasta have been divided into four hydrologic units: Sacramento River, McCloud River, The Whaleback-Ash Creek Butte depression, and Shasta Valley. The areas of greatest eruptive activity on the mountain have been the McCloud River and the Whaleback-Ash Creek Butte depression (Blodgett, 1996). However, the oldest and largest lahars have been identified by geologists on the south-southwest side of the mountain (Sacramento River Unit), where glaciers were present in cooler times but are now absent (Roberts, 2004). These drainages often retain morphological evidence of Pleistocene glaciation and have been ephemeral or inactive since the beginning of the Holocene (Roberts, 2004). Lahars associated with eruptive activity, flank collapse, or heavy precipitation events could flow down any drainage, regardless of the presence of glaciers. However, lahars generated in channels headed by glaciers have a higher volume potential during noneruptive periods and have occurred with a much higher frequency, presenting variable degrees of hazard to surrounding communities based on: available water source, local topography, and available debris in the channel area.

The most recent lahars from Mount Shasta have not been related to eruptive activity, but to climate fluctuations (Osterkamp et al., 1986). Mud Creek (on the south flank) and Whitney Creek (on the north flank) have produced most of the historic lahars and are also the most deeply incised canyons on the mountain (Figure 15). These historic lahars have occurred during mid to late summer, and their formation has been associated with warm air temperatures, glacial ablation and heavy precipitation. The history of debris flows on all major drainage channels of Mount Shasta was reconstructed by Hupp, Osterkamp and Thornton in 1987 by means of geologic and dendrochronologic

observations. The magnitude and frequency of these flows was discussed by Osterkamp, Hupp and Blodgett in 1986, and most recently, the characteristics of noneruptive debris flows were discussed in 1996 by Blodgett and others.

2.3 SITE SELECTION

The Mud and Whitney Creek drainages have been selected for this study due to the availability of volumetric data from well-studied historical debris flows. Investigations of the 1997 Whitney Creek debris flow (De la Fuente and Bachmann 1998) and the Mud Creek debris flows (Osterkamp et al., 1986; Miller, 1980; Hupp et al., 1987; Blodgett et al., 1996) provide a basis from which to calibrate the GIS-based predictive inundation model (LAHARZ) in order to estimate the likely extent of future lahars and their expected impact. As an added benefit, the selected sites provide an excellent opportunity to study two different triggering mechanisms for noneruptive debris flows as well as their shared flow and emplacement characteristics.

2.3.1 MUD CREEK (GEOMORPHOLOGY AND DEBRIS FLOW HISTORY)

Mud Creek has received more attention than any other stream on Mount Shasta due to the unusual series of debris flows that threatened the town of McCloud during the summers of 1924, 1925, 1926 and 1931, initiated by the breakup of Konwakiton glacier in response to low precipitation and intense summer warming trends (see Appendix A for historic photo series).

Mud Creek, the only perennially flowing stream, is the most deeply incised and longest of all Mount Shasta drainages as well as the most frequent site of lahar inundation on the mountain (Figure 4). It flows from the remnants of the Konwakiton Glacier

(translated "muddy" in the Wintu language by Sisson, 1884) on the southeast flank of Mount Shasta, to the McCloud River. Below the glacier, Mud Creek cuts through 200 m of the Mud-Ash debris fan, forming a steep-walled canyon. The fan covers an area of nearly 300 km², consisting mostly of pyroclastic flow deposits. Debris flow deposits are thickest in the upper reaches of the Mud-Ash fan and thin beyond recognition in some parts of the lower slopes (Osterkamp et al., 1986). When flow volumes are large enough to exceed lower fan infiltration capacity (Hupp, 1987), Mud Creek canyon discharges into the McCloud River, which joins the Pitt River before feeding into the Sacramento River and eventually, San Francisco Bay. This was the case when extreme glacial outburst floods (jökulhlaups) disintegrated the ice and bedrock, generating the massive debris flows from 1924 to 1931. These events caused the western overhanging terminus of the Konwakiton, calving into Mud Creek, to separate into a much smaller volume of ice which is now referred to as Mud Creek Glacier. Konwakiton Glacier now holds a relatively small volume of ice at 5.7 million m³ (Driedger and Kennard, 1986) but may owe its historic instability to a steep, erodible bed, and higher insolation on the South-facing slopes.

From Konwakiton Glacier, Mud Creek flows southeasterly before curving to the south and entering the McCloud River about 8km southeast of the town of McCloud. Due to its proximity to McCloud, Mud Creek basin is the only glacier-headed drainage of Mt Shasta that poses a serious threat to urban areas during periods of volcanic inactivity. The Mud Creek debris flows from 1924 to 1931 resulted in torrents of mud and boulders closing roads, washing out railways, and cutting off McCloud's main water supply. Though it did not enter McCloud, the 1924 debris flow produced a pulse of mud in the Sacramento River and its tributaries that was detected as far south as San Francisco Bay (Zanger, 1992).

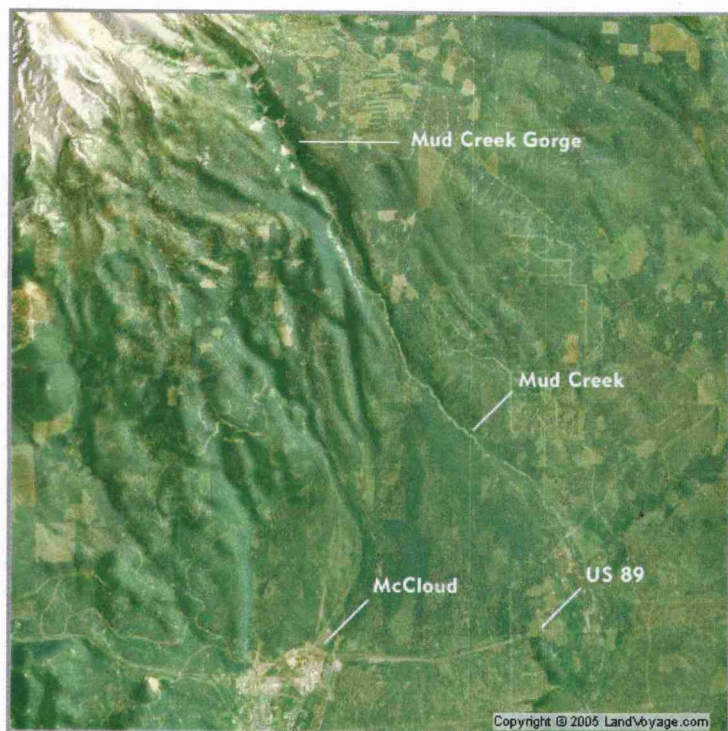


Figure 4 Mud Creek is the most deeply incised drainage on Mount Shasta, indicative of a history of high volume and frequency of debris flows from Konwakiton glacier. Mud Creek drainage rarely reaches the McCloud River, but the 1924 debris flow crossed US Highway 89 and made the connection.

(This Landsat 15m DEM drape taken from LandVoyage.com)

Several flows in 1924 lasting up to two weeks at a time deposited a total of 5.4 million m³ of debris, which covered over 6 km² near McCloud (Miller, 1980). The initial flow changed from seasonal to catastrophic on September 18, 1924, when 15 acres of pyroclastics bordering 13 km (8 mi) of steep Mud Creek Canyon walls collapsed, feeding the ongoing jökulhlaup with debris (Callahan, 2000). Witnesses described a very loud roar followed by huge clouds of dust and volcanic ash, which enveloped the mountain for hours and could be seen from 40 km (25 mi) away (San Francisco Chronicle, 1924 in Mount Shasta Companion, 2001). Clouds of dust, sometimes mistaken for eruptive activity, had been noted preceding mudflows on many other occasions (Mount Shasta Herald, 1936 in Mount Shasta Companion, 2001).

Investigations of these flows revealed at least four other lahars during the past 1200 yr that have covered large areas from McCloud eastward about 9 km and have

extended southward into the McCloud River (Osterkamp et al., 1986). The oldest identifiable Holocene lahar deposit forming the western side of the Mud Creek fan was mapped and dated by Dickson and Crocker (1954) following investigations of the 1924 – 1931 series, at about 1200 yr old (Hill and Egenhoff, 1976). Roberts (2004) suggests that the oldest Holocene lahar deposits forming the Mud Creek fan may have resulted from extreme glacial outburst floods during periods of warm and dry weather. Several of these flows occurred during the Little Ice Age and may have resulted from a combination of accelerated glacial growth and intense warming trends (Roberts, 2004). The two oldest lahars identified on the Mud Creek fan (dated at 600 and 1200 yr ago) are believed to have deposited significantly more debris than the later two (dated at 124 and 300 yr ago by Dickson & Crocker, 1953). The 1924 to 1931 series of flows, which together deposited an estimated $2.3 \times 10^7 \text{ m}^3$, may have been the smallest on the fan (Osterkamp et al., 1986). The larger flows would have transported a much larger percentage of their volume into the McCloud River. The assemblage of 1924 to 1931 lahars was the last to deposit large amounts of debris on the Mud Creek alluvial fan.

2.3.2 WHITNEY CREEK (GEOMORPHOLOGY AND DEBRIS FLOW HISTORY)

The northwest flank of Mount Shasta is drained by Whitney Creek and its main tributaries, Bolam and Graham Creeks. Glacial meltwater originates from Whitney and Bolam Glaciers and has deeply incised weak pyroclastic fan deposits 8 km from the summit to form Whitney and Bolam gorges. These prominent V-shaped gorges have steep, unvegetated 100-meter high walls of light colored, highly erodible pyroclastic deposits – a prime source area for debris flows. The Whitney-Bolam fan extends to the Shasta River, more than 20km from the summit of Mount Shasta. Miller (1980) estimated that during the last several hundred yr, many lahars traveled over 24 km from the summit to form an

extensive fan north and east of Lake Shastina. Only unusually high volume runoff events like these are able to reach the Shasta River, as most flows infiltrate the fan deposits (Osterkamp, 1986).

Whitney and Bolam creeks are seasonal and flow only during the summer when the glaciers are melting, or during heavy rains. The highest flows in the lower reaches usually occur at night as the afternoon peak flows take several hours to reach Highway 97, 14 km downstream. Whitney Glacier is the largest in California (Lewis, 1977 in Callaghan, 2000) and the only valley glacier on Mount Shasta lying adjacent to Bolam Glacier in the saddle between the Hotlum cone and Shastina. Whitney Creek begins at its terminus, at an elevation of 3100 m (Figure 5: A), and passes through incised glacial moraines down to 2600 m (B).

This area of unconsolidated, highly erodible moraines makes this a likely debris source area for future flows. In the next segment, from 2600 – 2140 m, the channel bed and walls are made up of resistant lava flows which function mainly as a transport reach for passing debris flows. At the lower end of this reach (2140 m - C) is Whitney Falls, where the creek cascades 100 m down into the head of Whitney Gorge. This area of incised pyroclastic fan deposit is capped by a 9,300-year-old andesite flow, which filled in some of the previously developed drainages (De la Fuente and Bachmann, 1998). This lava flow forms the western boundary of the gorge below Whitney Falls. The incision depth into the fan deposits decreases in the downstream direction. Below the end of the aggradational gorge area at an elevation of 1600 m (D), the channel incision is shallow, ranging from 3-12 m deep. Large flows that are well constrained in the upper channel are therefore free to spread out as they approach and pass U.S. Highway 97 (E). This

accounts for the tendency of high-risk zones along stream channels to widen in the downstream direction.

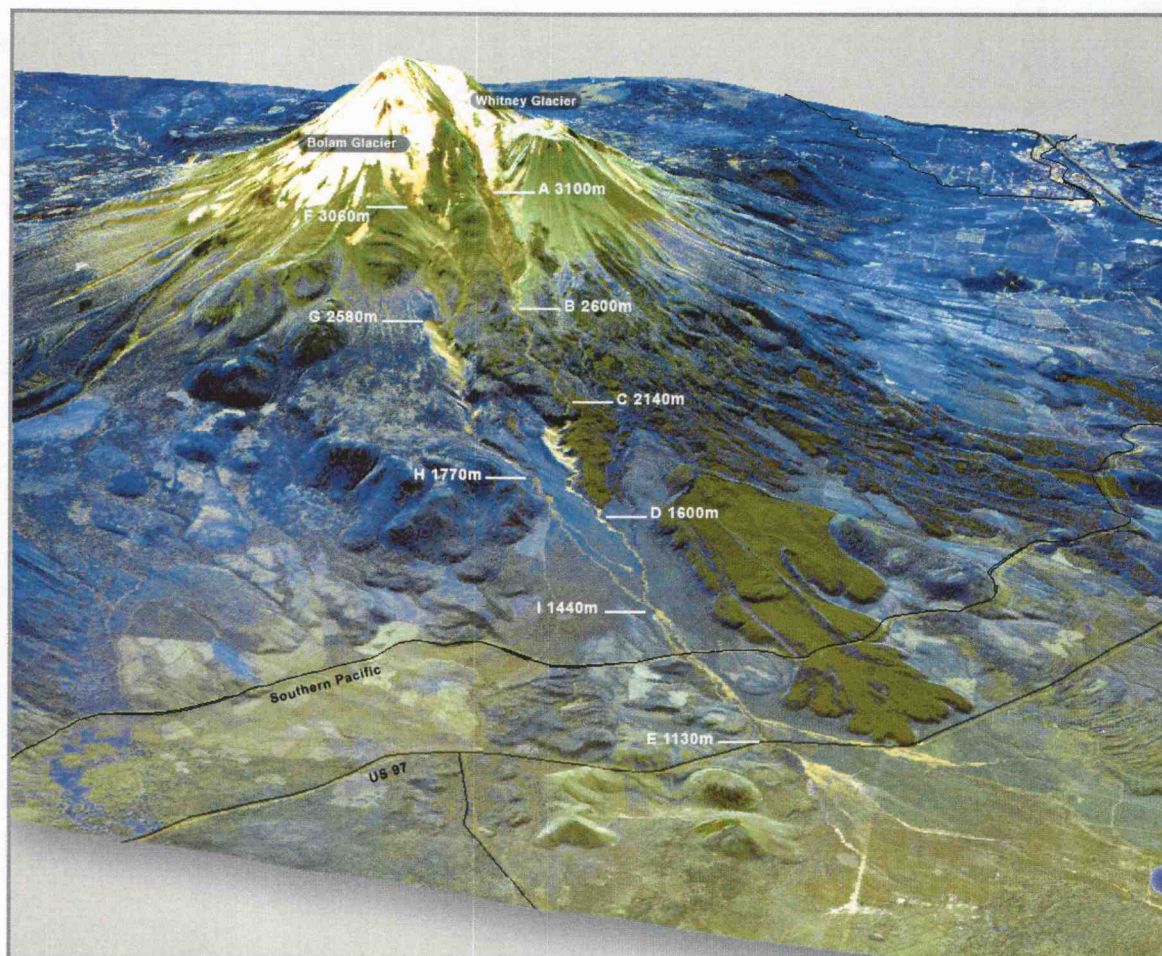


Figure 5 Elevations of key features in the geomorphology of Whitney and Bolam Creek drainages on the northeastern flank of Mount Shasta. Data shown is ASTER VNIR composite taken September 2001, draped over a USGS 10m DEM.

The geomorphology of the Bolam Creek tributary is similar. It emerges from two locations at the terminus of Bolam Glacier at an elevation of 3060 m (F). The two forks of Bolam Creek flow through glacial moraines, and a mixture of pyroclastic deposits and lava flows before the main (east fork) stem flows over the 30 meter-high Coquette Falls at an elevation of 2580 m (G). From here, they cascade into the head of Bolam Gorge to a

maximum incision depth of 140 m. Below 1770 m (H), a shallow incision allows for debris flow diversions. Bolam Creek and Whitney Creek converge at an elevation of 1440 m (I) on the lower fan (De la Fuente and Bachmann, 1998). Below the confluence, a 5 km reach of Whitney Creek flows on fan deposits that are restricted to a width of less than 2 km by adjacent lava flows. Below this constriction, the Whitney-Bolam debris fan widens to nearly 4 km and extends to the Shasta River valley, near Lake Shastina, where fan deposits become interbedded with fluvial sediments of the river (Osterkamp, 1986). Water from Whitney Creek is infiltrated into the fan deposits and underlying basalt to reappear as seepage and springflow in or near the Shasta River.

An investigation into the debris flow history of Whitney Creek by Hupp et al. (1987) found dendrochronologic evidence for at least 14 debris flows of different sizes; (1) large flows, having long runout distances (to approximately 27 km from the summit) with considerable over-bank deposition (1670, 1840, 1935, 1985); (2) medium flows, having limited runout distances (to approximately 18 km from the summit) with some evidence of out-of-bank flow (1705, 1790, 1804, 1830, 1868, 1919); and (3) small in-channel events (1908, 1952, 1960, 1974, 1977). This resulted in a frequency of 4.8 per century. A more recent study by De la Fuente and Bachmann (1998) of the large 1997 Whitney Creek debris flow discusses the characteristics of debris flows since 1990. Of these flows, the greatest occurred in 1935 and closed both Highway 97 and the Southern Pacific Railroad, depositing an estimated $4.0 \times 10^6 \text{ m}^3$ of debris over approximately 8 km^2 of the lower fan (Osterkamp et al., 1987). The flows of 1985, 1997, 1994, and 1996 (in descending order of magnitude) along with all other historic debris flows in Whitney Creek have occurred in July or August, usually after temperature increases. The largest debris flows have in common the additional contributing factor of intense convective precipitation (Blodgett et al., 1996; De la Fuente and Bachmann, 1998). If the 1935 lahar is representative of large flows for

Whitney Creek, intermediate-sized flows reaching up to 18 km from the summit may have had volumes of up to $2.5 \times 10^6 \text{ m}^3$.

2.4 LITERATURE REVIEW AND LAHAR VOLUME RECONSTRUCTION

In the following section (2.4), debris flow data from various published and unpublished sources pertaining to lahars from Mud, Whitney and Big Canyon Creeks are reviewed in order to determine the magnitude of lahars that have been generated on Mount Shasta. As the magnitude, frequency, and behavior of past lahars is the basis for predictive modeling, it is important to look at the volumetric evidence left by various categories of lahars. The field component of this study consisted of the inspection of key lahar deposits considered to be representative of various size classes of lahars from Mount Shasta in order to verify published volume estimates and reconstruct volumes in cases where there were none available. The volumes of the Whitney Creek lahars of 1935, 1985, and 1997, and the Mud Creek lahars from 1921 – 1934, were obtained from literature. An estimated volume for the Big Canyon Creek lahar was derived from unpublished sources and from field observations.

2.4.1 WHITNEY CREEK LAHARS OF 1935, 1985 AND 1997

Studies related to the Whitney Creek Lahars of 1935, 1985, and 1997 were reviewed in order to get a range of volumes indicative of the likely magnitude and frequency of future flows. As mentioned above, the largest of these flows (1935) had a volume of approximately $4.0 \times 10^6 \text{ m}^3$. Data on its depositional area were not found, but it is likely to have had a runout distance similar to that of the flow of 1985 (27 km, based on Osterkamp et al., 1996). Based on observations at soil pits and other sites on the lower

Whitney-Bolam fan, the same study found that the 1935 debris flow covered an area of about 8 km² to an average depth of 0.5 m.

The much smaller flows of 1985 and 1997 were found to share a similar deposition area and runout distance, as evidenced by Figure 6. The 1985 area plotted by Blodgett et al. (1996) and the deposition area derived from an air photo of the 1997 flow were found to be about 1,875,000 m² and 1,212,000 m² respectively. The reported depth of the 1985 deposit on the fan ranges from 0.4 to 2.5 m, decreasing in the downstream direction and averaging 1 m. This would indicate approximate volumes of 1.8×10^6 m³ for the 1985 flow and 1.2×10^6 m³ for the 1997 flow. Both flows shared a similar pattern of travel and deposition. They were mostly confined to the channel from the initiation point at the terminus of Whitney and Bolam glaciers, to just below the U.S. 97 highway bridge, from where they spread across the Whitney-Bolam fan down to Juniper Flat.

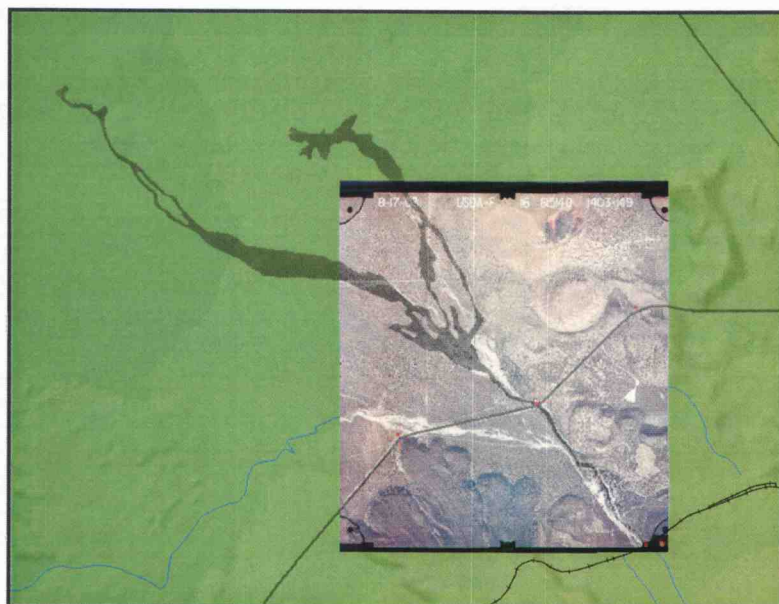


Figure 6. Air photo of 1997 Whitney Creek debris flow shown with a vector overlay of the extent of the 1985 debris flow mapped by Blodgett et al., 1996.

Boulder-covered levees and scarring on pines growing near the peak flow height were indicators of a depth of flow ranging from 5 to 10 m for the 1985 flow (Hupp et al., 1987). The same evidence was seen in the field for the 1997 flow (Figure 7). Mud lines for the 1985 flow were reported to reach up to one meter from the top of the culvert at Highway 97 (De la Fuente and Bachmann, 1998). Slightly lower mud lines were seen in the culvert for the 1997 event (Figure 8). The main difference between the two flows was that the 1997 flow was diverted before reaching the fan and flowed over the highway 700 m to the West.

An intermediate volume of $1.5 \times 10^6 \text{ m}^3$ derived from the 1985 and 1997 flows is considered to be representative of the smallest lahar size (class 1) able to reach beyond the proximal hazard zone. These flows occur more frequently than once every 15 yr, as indicated by analysis by Osterkamp et al. (1986), and are included in the area of highest risk of lahar inundation. A second size class is set at $5.0 \times 10^6 \text{ m}^3$. It is derived from the volumes of the Whitney Creek 1935 event ($4.0 \times 10^6 \text{ m}^3$) and the 1924 Mud Creek event ($5.4 \times 10^6 \text{ m}^3$). Lahars of this magnitude are assumed to occur somewhat less frequently than the "class 1" lahars do.



Figure 7. Photo of Whitney Creek, right bank boulder levee downstream from the US97 culvert. Scarring on buried pines indicates peak flow depth.

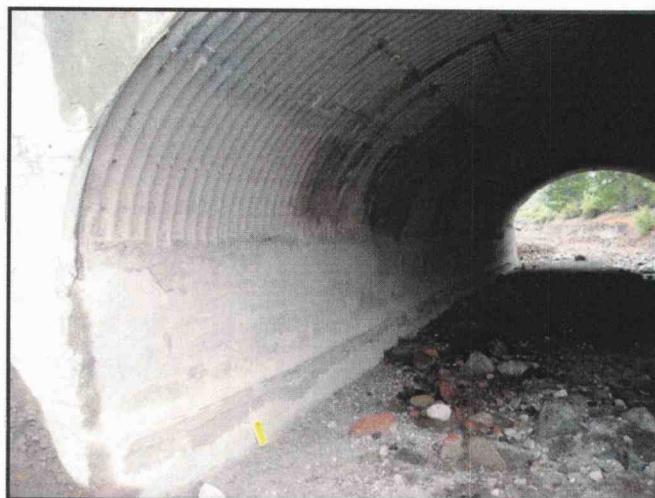


Figure 8. Mud lines as seen in the US97 culvert indicating the height of wave crests during the 1997 Whitney Creek debris flow.

2.4.2 MUD CREEK LAHARS OF 1924 – 1931

The volume of the historic Mud Creek lahars is well established, yet difficult to verify. In a study by Wood immediately after the 1931 debris flow (from Hill and Egenhoff, 1976), volume estimates were made for deposited debris as well as amounts reaching the McCloud and Sacramento rivers (Table 1).

Table 1. Amount of debris from the 1924–1931 debris flows from Konwakiton Glacier, Mount Shasta, California. Data is from Hill and Egenhoff (1976).

Year	On Debris Fan	Into McCloud	Into Sacramento River
1924	7,000,000	1 - 3,000,000	---
1925	small	300,000	normal streamflow
1926	1,300,000	700,000	700,000
1931	18,000,000	1,000,000	1,000,000
Total	26,300,000	3 – 6,000,000	1,700,000

Grand total: 23,701,200 - 25,994,865 m³ * original data given in cubic yards

These data were compared to the volume derived from an aerial photo mosaic from 1944. As with the Whitney Creek flow deposits, polygons were created using ESRI ArcMap functions from the georeferenced deposit area. Area attributes were then added to the shapefile, and statistics calculations were added for a total. Results are estimates due to manual georeferencing, digitizing, and the use of an average deposit thickness for the area of obvious deposition in the air photo.

In the case of the Mud Creek series of lahars, an estimation of the total affected area, from all flows from 1924 to 1931 was of interest. The area calculated from this 1944 air photo was about 5,614,000 m², (Figure 7). If the average thickness of 0.98 m suggested by Osterkamp is used, the resulting volume is about 5,500,000 m³. This estimate corresponds with the reported volume of the 1924 flow, but falls short of the reported 23 million m³ for the entire 1924 – 1931 period. There are several possible reasons for this volume discrepancy: (1) Only 13.7×10^6 m³ were reported by Wood (1931) in Hill and Egenhoff (1976) to have deposited on the debris fan. The remaining volume was transported as hyperconcentrated flow and stremflow into the McCloud river and beyond (Table 1); (2) The deposition area recognizable from the air photo of 1944 may not be a good representation of the entire affected area, as parts of it infiltrated the surrounding forest; (3) The deposit thickness was greatest (up to 4 m – see Photo 14, Appendix A) near the stream channel and reduced gradually as it spread out over the fan. The assumed average thickness of 0.98 m may need to be increased to represent the actual variability in deposit height above the pre-1924 fan surface. Despite this discrepancy, the 1944 air photo was used to compare relative runout distance of the 1924 flow with the modeled flow.

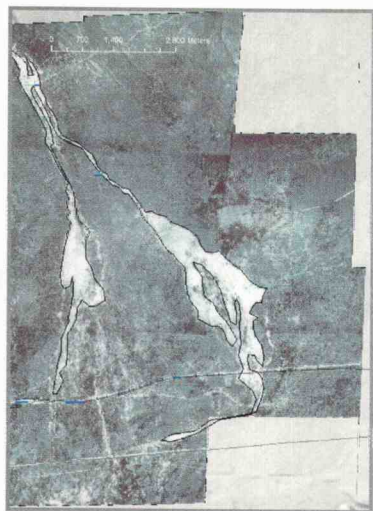


Figure 9 1944 Air photo provided by the USFS McCloud Ranger Station of 1924-1931 Mud Creek debris flow shown with a vector outline of approximate extent for an area calculation.

The volume of $2.3 \times 10^7 \text{ m}^3$ is taken as representative of class 3 lahars for Mount Shasta. Since 1881, debris flows have occurred along Mud Creek in at least 8 yr, indicating a frequency during recent centuries of about one per decade. Of these, only five large magnitude flows (including the series of 1924 – 1931) have occurred during the last 1200 yr, resulting in a recurrence interval of about 250 yr for these events. This magnitude category corresponds to a medium risk inundation area for hazard mapping purposes.

2.4.3 BIG CANYON CREEK LAHAR

In the Big Canyon Creek drainage on the South flank of Mount Shasta, Roberts (2004) found evidence of a large, cohesive lahar possibly related to the 40 km^3 debris avalanche which occurred on the northwest side of ancestral Mount Shasta (Crandell, 1989), creating the hummocky topography currently seen in Shasta Valley. Dated at over 300,000 yr ago, this avalanche could have coincided with an eruption. The Big Canyon Creek lahar was found to be similar in age to the avalanche, and containing a significant amount of pumice, indicating that an eruption most likely occurred prior to or coincident

with the avalanche (Roberts, 2004). In fact, the study found that matrix samples of the debris avalanche in Shasta Valley revealed similar clay content and color as the lower Big Canyon Creek lahar. Debris avalanches are known to transform into lahars through disintegration of avalanche blocks. High clay and water content in the avalanche matrix creates a cohesive lahar capable of traveling long distances. Volumes for this type of lahar have been estimated at up to 4 km³ (Vallance and Scott, 1997). For modeling runout distances of debris avalanches larger than 1 km³, Crandel (1989) has recommended using a design volume of 1 km³ in estimating potential hazards from debris avalanche or flank collapse. A coefficient ($f = 0.075$) derived from height-to-length ratios of various volcanic debris avalanches of this magnitude can be multiplied by the elevation difference between the summit and points 20 km downslope from it to predict runout distances of debris avalanches. However, lahars transformed from these catastrophic events can travel much further.

No modern glacier exists above Big Canyon Creek, but there is evidence for at least one Pleistocene glaciation, which would have provided the large amount of water required to mobilize it into distal areas. The lahar deposits of Big Canyon Creek are among the oldest found on Mount Shasta. These deposits can be seen on open outcrops near the town of Mount Shasta, along California Highway 89 and Interstate Highway 5 (Figure 10).

The approximate boundaries of these surfaces were mapped by Roberts (2004) based on soil pits, road-cuts, and geomorphic features. Due to difficulty in locating good exposures, the extent of the deposit is thought to be much larger than the area mapped. The boulders characteristic of this deposit are coarse-grained andesites that have undergone significant weathering, retaining a coating of silt and clay. During field inspection of the lahar deposit, this category of boulders was seen throughout portions of

Mount Shasta City and beyond I-5 toward Siskiyou Lake, well beyond the extent of mapped deposition.

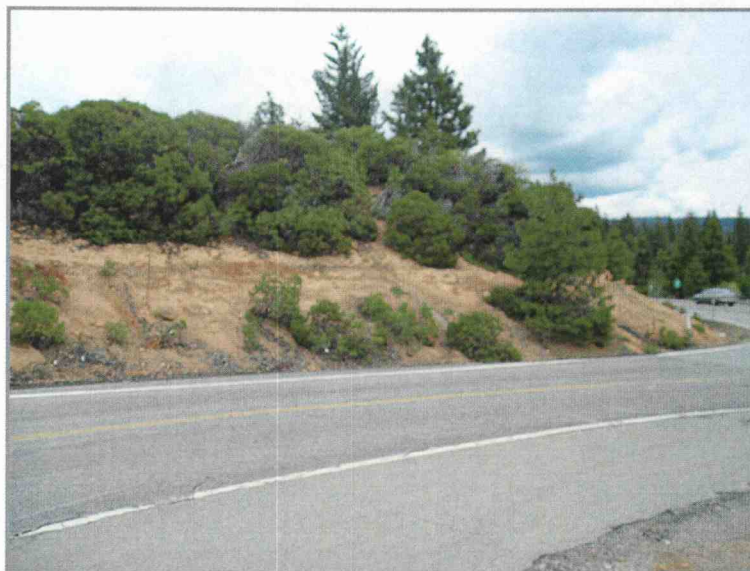


Figure 10. A roadcut exposing > 2m thick deposits of the Big Canyon Creek lahar in the study area.

The area of the Big Canyon Creek lahar was digitized and georeferenced (Figure 11) with an area calculation of 7,488,272 m². The volume of the lahar, based on field observations of general extent and an average thickness of 1.5 – 2 m, is estimated to be from 5.0 to 7.0 x 10⁷ m³ (Scott, pers. comm., 2005). Although it is unclear where the lahar was initiated on the edifice of ancestral Mount Shasta, the mapped area probably delineates a portion of the debris fan apex, as other parts are buried by younger Holocene deposits. If this is true, the lahar could have easily extended as far as Dunsmuir to the South, and Siskiyou Lake, southwest of the I-5 crossing point (Roberts, pers. comm., 2005). This assumption was modeled with a volume of 7.0 x 10⁷ m³ and found to be feasible over the present drainage topography (Figure 11). A volume assumption of 7.0 x 10⁷ m³ would indicate that the unmapped area is 4.6 times larger than what is shown

(taking an average thickness of 2 m).

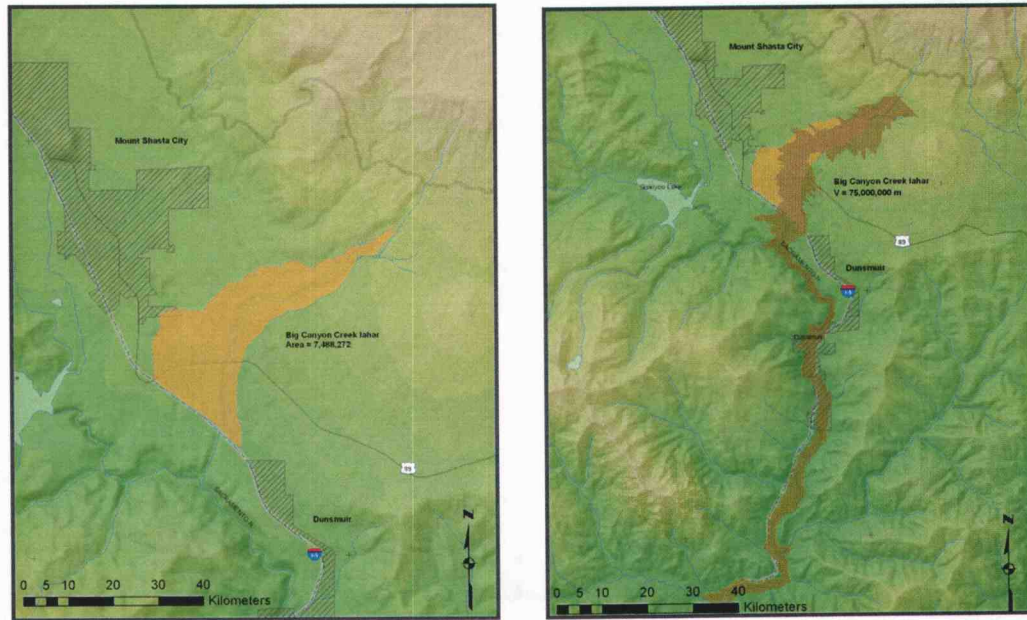


Figure 11 The area of the Big Canyon Creek lahar mapped by Roberts ,2003 (left) and the path part of it may have taken if a volume close to $7.0 \times 10^7 \text{ m}^3$ is assumed (right).

Based on the existence of the Big Canyon Creek lahar deposit, a fourth size class of $7.0 \times 10^7 \text{ m}^3$ is defined for modeling purposes. Lahars of this magnitude are grouped into the low risk, high consequence category, as the conditions for their generation exist only in the scenario of a flank collapse or pyroclastic eruption.

3. METHODS

3.1 DATA COLLECTION

The data used in this study included a DEM (30 m grid size from USGS 7.5 minute quadrangles), air photos of Mud (1944) and Whitney (2000 and 2001) Creeks, historical records and photos of the 1924 – 1931 Mud Creek debris flows (Hill and Egenhoff, 1976 and others), reports from investigations of the 1997 Whitney Creek debris flow (De la Fuente and Bachmann, 1997), a 2001 ASTER visible and near infrared (VNIR) 3-band composite image, lahar deposit delineations derived from unpublished geological maps of Mount Shasta (Roberts, 2004), a chronological study of events at Mount Shasta in the past 10,000 yr (Miller, 1980), and volcanic hazard maps developed by Osterkamp et al. (1986) and Miller (1980). Air photos and reports of the 1997 event were obtained from the USFS McCloud Ranger Station. Certain documents which are no longer in publication, such as the report by Miller (1980) and a pamphlet on volcano hazards at Mount Shasta, were obtained from the USGS Cascades Volcano Observatory. The report and map by Osterkamp et al. (1986) was obtained from the Valley Library at Oregon State University. Additional sources of data in digital format, such as shapefiles of California hydrography, roads, watersheds, railroads, and cities were downloaded from the California Spatial Information Library at <http://gis.ca.gov>. The Mount Shasta Collection in the Library of the College of the Siskiyous, Weed, California was a source for online access to historic photographs and reports of the Mud Creek debris flows of 1924 to 1931.

These available resources were used in conjunction with field observations in order to gain a better understanding of the topography affecting flow patterns, the nature of deposited sediments, and morphological evidence of lahar volume, behavior and characteristics in proximal and distal areas. Inspection of various deposits on the alluvial

fans of the study area verified volume estimates made by others in the case of Mud and Whitney Creeks (Wood, 1931 in Hill and Egenhoff, 1976; Miller, 1980; Osterkamp et al., 1986) and allowed for an initial estimate of a volume for the Big Canyon Creek lahar identified by Roberts (2004).

3.2 MODEL CALIBRATION AND IMPLEMENTATION

3.2.1 LAHARZ OVERVIEW

LAHARZ was chosen as the means for estimating areas of potential lahar inundation in the two most historically flooded drainages of Mount Shasta: Mud Creek and Whitney Creek. The methodology has been used to consistently map lahar-inundation hazards for Cascade stratovolcanoes as well as several Latin American sites. Based on historic records and geologic mapping of flow deposits on Mount Shasta, a range of potential volumes were estimated for future flows along Mud and Whitney Creek. LAHARZ uses these volumes, a DEM, and a set of statistically derived empirical equations to predict the valley cross-sectional area (A), and the planimetric area (B) inundated by each simulated lahar (Figure 12) (Iverson et al., 1998). For user-selected drainages and user-specified lahar volumes, LAHARZ calculates expected deposit geometry within the cell-based GRID portion of ARC/INFO and delineates a set of nested lahar-inundation zones depicting gradations in hazard level for lahars of increasing volume and decreasing probability. These inundation zone grids can be plotted with other data themes in a GIS environment to cartographically represent that the hazard potential is highest near volcanoes and along stream channels, and diminish gradually as distance from the volcano and elevations above the valley floor increase.

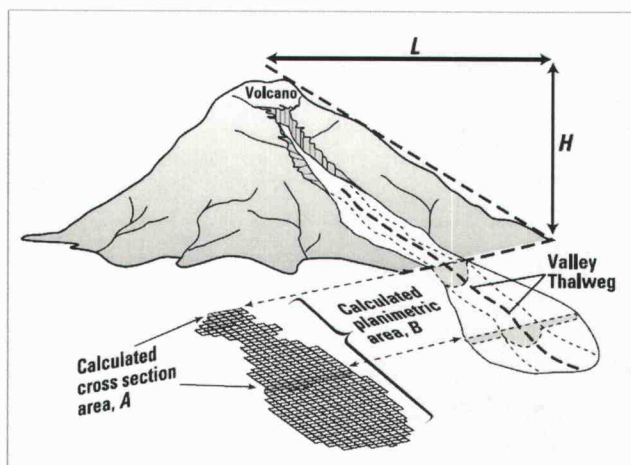


Figure 12 Diagram of association between dimensions of an idealized lahar and cross-sectional (A) and planimetric (B) areas calculated by LAHARZ for a hypothetical volcano. The ratio of vertical drop (H) to horizontal runout distance (L) describes the extent of proximal volcano hazard. LAHARZ begins calculations of lahar-inundation hazard zones where a user-specified stream and the proximal-hazard zone boundary intersect. Modified from Schilling (1998).

Driving the model are a set of predictive equations which provide all the information necessary to calculate and plot inundation limits on topographic maps:

$$(1) A = 0.05V^{2/3} \quad (2) B = 200V^{2/3}$$

These equations were developed by Iverson et al. (1998) from statistical analysis of 27 lahar paths at nine volcanoes and calibrated from scaling analysis of lahar kinematics to estimate cross-sectional (lateral) and planimetric (downstream) areas as functions of lahar volumes (Schilling, 1998). These relationships were derived from analysis of a wide range of lahar volumes ranging from the $4.0 \times 10^9 \text{ m}^3$ Osceola mudflow of Mount Rainier, to the 10 m^3 experimental debris flows generated at the U.S. Geological Survey debris-flow flume in the H.J. Andrews Experimental Forest. The analysis resulted in equations that effectively constrain the rate at which width and length of a hazard zone planimetric area increases as lahar volume increases. Despite their limitations (see the discussion section), and the variability possible in lahar characteristics, the equations represent the statistical similarity in the depositional geometry of most lahars (A and B) and, combined with a DEM,

they are useful guidelines for forecasting areas subject to inundation by lahars of various volumes (Iverson et al., 1998).

Input data required by the model include a depressionless DEM, derived supplementary surface hydrology grids, specified lahar volumes, specified upstream flow initiation point, and a specified H/L value for the identification of the proximal hazard zone boundary (PHZB).

3.2.2 LAHARZ IMPLEMENTATION

LAHARZ was developed as a set of Arc Macro Language (AML) scripts running within the cell-based GRID portion of ArcInfo. Its successful use requires an understanding of DEMs, the ArcInfo GRID module, and the H/L ratio from the energy cone concept. The algorithm and processing sequence are described in Appendix 1. The major steps taken to generate lahar inundation hazard zones for selected Mount Shasta watersheds are described below.

3.2.2.1 DEM PREPARATION

A collection of 7.5 minute USGS 7.5-Minute DEMs covering Mount Shasta and vicinity were acquired from the USGS EROS Data Center web portal corresponding to the USGS 1:24,000- and 1:25,000-scale topographic quadrangle maps. These files were stitched together using ArcInfo to remove quadrangle data gaps at the seams. The resulting DEM format with a grid spacing of 30 m was then converted to raster format using the "DEM to Raster" ArcToolbox procedure and reprojected to its native Universal Transverse Mercator (UTM) Zone 10 projection and referenced to the North American

Datum (NAD) of 1927 (NAD27). Elevation units are in m relative to the National Geodetic Vertical Datum of 1929 (NGVD 29).

The first procedure executed within LAHARZ was the removal or "filling" of sinks present in the DEM which could inhibit surface flow routing. A detailed DEM is desirable in order to predict the behavior of a lahar in relation to subtle topographic variations in areas of low relief. For the purposes of this study, a 30m grid size DEM was considered adequate for reasons stated in the discussion section.

3.2.2.2 SURFACE HYDROLOGY GRID GENERATION

Several GRID surface hydrology functions were used within LAHARZ to derive flow direction, flow accumulation, and stream delineation grids from the DEM. An accurate identification of stream patterns is a critical step in inundation area calculations. This is done by adjusting the user-defined stream-delineation threshold value (from a LAHARZ default of 1000 cells) if needed. If the number of cells 'flowing into' an individual cell exceeds the threshold number, then the cell is defined as being a part of one of the flow paths. The flow direction function calculates the direction of flow out of every cell in the DEM and stores them in a flow direction grid. The flow accumulation function creates a flow accumulation grid and, using values in the flow direction grid, assigns each cell in the flow accumulation grid a value that is the sum of the number of cells that flow into it. LAHARZ then identifies cells in the flow accumulation grid having values greater than a user-specified, stream-delineation threshold and stores those cell locations in a stream grid. Two stream threshold values were used and inspected for relative accuracy in the representation of known flow initiation areas. The threshold value of 1000 was considered adequate for the identification of Mud and Whitney Creek channels within the proximal

hazard zone.

3.2.2.3 CALIBRATION AND PROXIMAL HAZARD ZONE DELINEATION

The proximal hazard zone boundary (PHZB) is the area of greatest hazard surrounding a volcano which is most likely to be affected by primary volcanoclastic flows, such as pyroclastic flows and debris avalanches. The hazards that typically extend beyond this boundary to distal areas are lahars and ash fall. The model assumes that source areas for lahars are within a proximal hazard zone defined by the intersection of an "energy cone" with the topographic surface of the volcano (Malin and Sheridan, 1982). Also known as energy-line, mobility, or H/L cones, these features have slopes that describe the extent of "primary" deposits left around a volcano. Volcanologists have used them as a way to describe the potential runout distances of debris avalanches or pyroclastic flows that initiate at the summit or on volcano flanks (Hayashi and Self, 1992). These cones usually have an apex coinciding with the volcano summit and a slope determined by a ratio of vertical drop (H) to horizontal runout distance (L). LAHARZ uses the H/L ratio to define the PHZB (Figure 10). Typical ranges of H/L values that define proximal hazard zones are about 0.1 to 0.3 depending on the size and type of flow event (Schilling, 1998). LAHARZ assumes that lahar inundation begins at the boundary of the proximal hazard zone and continues downstream to distal areas until all volume has been deposited (Iverson et al., 1998). The deposits of small in-channel lahars will be confined to this zone but the volume of a distal lahar will exit the proximal hazard zone to a distance constrained by the empirical equations and by valley topography.

Model calibration, therefore, consists of adjusting the H/L values to the point where the PHZB surrounding the volcano corresponds with the beginning of lahar deposition for a

given drainage, allowing the model to delineate inundation areas which match the extent of known deposits as closely as possible. Depending on the topography, large lahars may begin over-bank flow and deposition much earlier than small in-channel lahars, but will travel much further downvalley. Large-volume lahars, such as the Osceola ($4.0 \times 10^9 \text{ m}^3$) or Electron ($2.5 \times 10^8 \text{ m}^3$) at Mount Rainier, have been modeled by Iverson et al. (1998) with a H/L value of 0.23, resulting in a proximal hazard zone that extends to a radius of about 20km from the summit. In the case of Mount Rainier, it is assumed that only the rare flows larger than 10^7 m^3 will pose significant hazards outside of this PHZB.

On Mount Shasta, the most adequate location of the PHZB was found to be approximately 10.5 km from the summit cone. Along Mud Creek, it corresponds with the location of the Mud Creek Dam built after the 1924 debris flow. This radial boundary, on most drainages around the volcano (including the Whitney/Bolam drainage) intersects the debris fan apex, where flows transition from erosional to depositional, as seen in previous studies (Osterkamp et al., 1986; Blodgett et al., 1996; De la Fuente and Bachmann, 1998) and aerial photos. The extent of the proximal hazard zone for Mount Shasta is represented by an H/L value of 0.26, in which H is the elevation difference between the summit and the hazard boundary line and L is the horizontal distance from the center of the summit cone to the hazard boundary line.

Adjusting the H/L energy cone ratio will shift the boundary and accordingly modify the upstream and downstream limits of the computerized distal lahar hazard zones, but will not affect the lateral limits of these zones. Therefore, the methodology is robust with respect to uncertainty in the extent of the proximal hazard zone (Iverson et al., 1998).

3.2.2.4 FLOW VOLUME SELECTION

A range of possible lahar volumes were selected for Mud and Whitney Creek drainages to represent various categories of historic and pre-historic flows from Mount Shasta. For the purpose of comparing modeled runout distance and planimetric area to mapped and documented flows in Whitney and Mud Creek drainages, the known lahar volumes for each drainage were used: for Whitney Creek, $1.5 \times 10^6 \text{ m}^3$ and $4.0 \times 10^6 \text{ m}^3$; for Mud Creek, $5.4 \times 10^6 \text{ m}^3$ and $2.3 \times 10^7 \text{ m}^3$. As described above, for the purpose of mapping inundation hazard areas with uniform distributions, design volumes of 1.5×10^6 , 5.0×10^6 , 2.3×10^7 , and $7.0 \times 10^7 \text{ m}^3$ were extrapolated to both drainages to represent possible lahar size classes based on historical records and geologic mapping.

The smallest volume used, $1.5 \times 10^6 \text{ m}^3$, is representative of the smallest flows in Mud Creek between 1924 and 1931, as well as the decadal flows of 1985 and 1997 in Whitney Creek. The next volume used, $5.4 \times 10^6 \text{ m}^3$, corresponds to the 1924 Mud Creek debris flow generated by the disintegration of Konwakiton Glacier. An intermediate volume used, $2.3 \times 10^7 \text{ m}^3$, corresponds to the total volume deposited along Mud Creek during the sequence of flows from 1924 to 1931. Although the Whitney and Bolam glaciers have historically been more stable than the Konwakiton, they are much larger and capable of generating flows of this magnitude by mechanisms of glacier outburst flooding, ice avalanching, and/or collapse of steep debris accumulation areas or debris-dammed channel levees. This magnitude could also be indicative of lahar generation by hot eruptive products melting ice and seasonal snowpack. A much larger volume, representing the low probability, low frequency, and high consequence hazard range, is derived from the Pleistocene "Big Canyon Creek Lahar" described above. This volume class is taken as

representative of lahars triggered by flank collapse or debris avalanche scenarios. These volumes were used as model input representing lahars of various origins and frequencies that have been known to occur on Mount Shasta.

4. RESULTS

The lahar hazard zonation map produced (Appendix E) shows the areas that have the highest risk of inundation by lahars generated on the northwestern and southeastern flanks of Mount Shasta. The hazard map is divided into two distinct hazard zones: 1) the proximal hazard zone, and 2) the distal hazard zone. The proximal hazard zone, outlined as a circle around the main edifice, is approximately 10.5 km from the summit and encompasses areas that could be affected by slope failures, debris avalanches, pyroclastic flows, and lahars originating on the volcano. Lahars originate within this zone and, having sufficient volume, are likely to travel beyond its limits onto depositional fan surfaces. The distal color-coded hazard zones delineated for Mud and Whitney Creek fans can be interpreted in terms of a qualitative gradation of hazard potential from "high risk" in areas most frequently affected by lahars, to "low risk" in distal areas affected only by low-probability, high-consequence events. The inundation hazard is greatest in stream channels close to the volcano and diminishes as elevations above valley floors and distances from the volcano increase.

4.1 HAZARD ZONES FOR THE WHITNEY CREEK DEBRIS FAN

The first lahar hazard zonation map included in Appendix E shows areas that may be affected by future lahars generated above Whitney Creek and its two tributaries, Bolam and Graham Creeks. Based on a range of possible lahar volumes indicative of local flow

deposits and extrapolated from volumes in other Mount Shasta drainages, the predicted planimetric areas subject to lahar inundation from Whitney Creek are shown below (Figure 13). These automated DEM-based hazard zone predictions are compared to (1) aerial photography of the 1985 Whitney Creek lahar (Figure 13, inset) and (2) mapped areas of debris flow hazard by (Osterkamp et al., 1986) based on dendrogeomorphic field evidence (Figure 14).

Table 2 shows the resulting inundation area and runout distance (from the summit) for the four volume classes modeled with LAHARZ. The smallest projected lahar has a volume close to that of the Whitney Creek 1985 lahar derived from aerial photography (Figure 13, inset). However, the deposits are seen to be distributed quite differently. The 1985 flow owes its great runout distance of about 22 km (compared to 16 km for the modeled flow) to diversion over the debris fan and eventual transformation into a hyperconcentrated flow. The areas where known diversion has occurred are shown as very irregular or jagged zone boundaries in the LAHARZ output. Such features are a reflection of irregularity in the local topography where valley walls are no longer able to constrain the planimetric area in a consistent way.

Table 2. Approximate inundation area and runout distance for modeled lahars from Whitney Creek.

Lahar Name	Est. Volume	LZ Area	LZ Distance
Whitney 1	 $1.5 \times 10^6 \text{ m}^3$	2.64 km ²	16.3 km
Whitney 2	 $5.0 \times 10^6 \text{ m}^3$	5.85 km ²	18.7 km
Whitney 3	 $2.3 \times 10^7 \text{ m}^3$	16.17 km ²	23.3 km
Whitney 4	 $7.0 \times 10^7 \text{ m}^3$	34 km ²	32.2 km

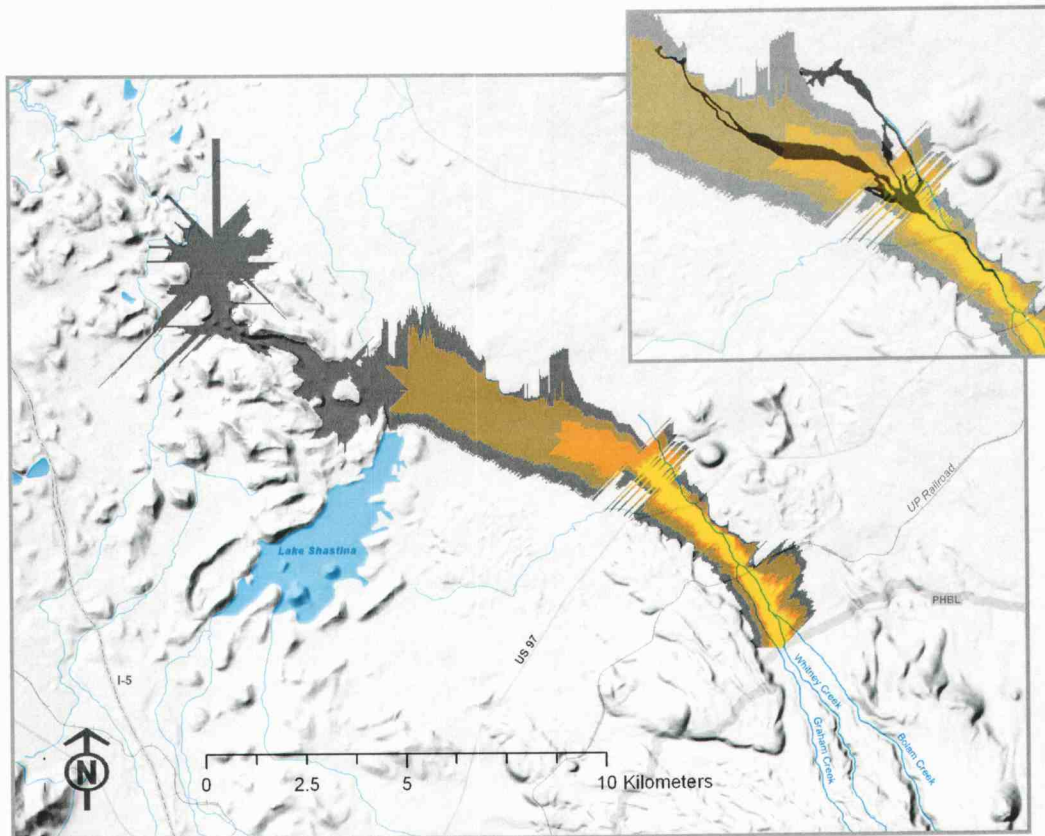


Figure 13 Resulting distal lahar hazard zones for the Whitney-Bolam debris fan. The inset shows an overlay of the approximate area of the 1985 Whitney Creek debris flow as outlined by Blodgett et al., 1996.

Areas of the hazard zone that “jut out” in one particular direction are an indication of the predicted flow direction based on the resolution of the topographic information used as input. In the case of the diversion area seen in the plotted 1985 inundation coverage (shown in black, Figure 13 inset), LAHARZ has reacted to the local topography by spreading the planimetric area in both directions (SW and NE). The area mapped by Osterkamp et al. (1986) showing debris flow hazard zones in the Whitney Creek drainage appears to be a better match to the LAHARZ-generated areas (Figure 14). The class 3 and 4 lahars modeled are shown to reach the northern end of the Shastina Lake.

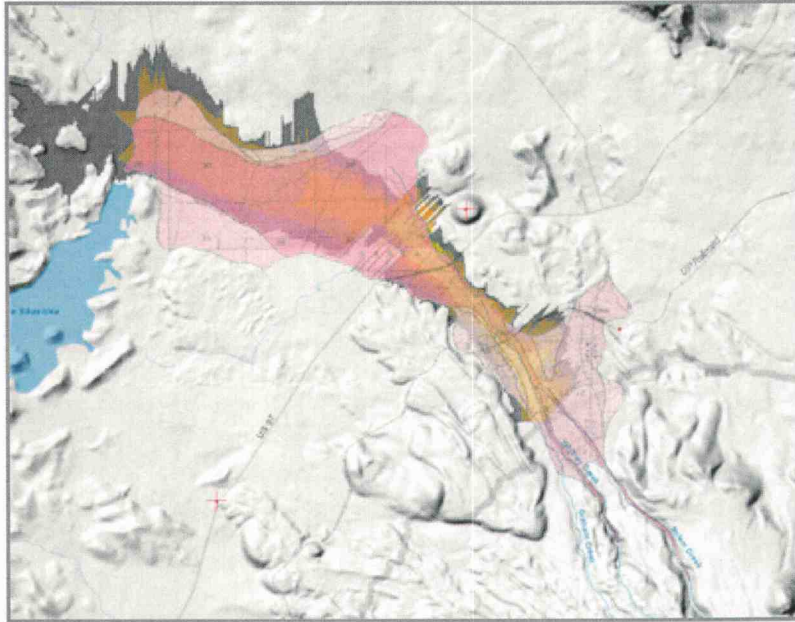


Figure 14 Overlay of the Whitney Creek portion of the hazard map by Osterkamp et al., 1986 showing hazard zone gradations related to the probability that a given area will be affected by debris flow activity within the next 100 yr. The high risk areas of most frequent activity are shown in darker color and the risk decreases progressively to lighter colors.

4.2 HAZARD ZONES FOR THE MUD CREEK DEBRIS FAN

The second lahar hazard zonation map included in Appendix E shows areas that may be affected by future lahars generated on the southeast flank of the Hotlum cone or at the terminus of the Konwakiton glacier. Based on a range of possible lahar volumes indicative of local flow deposits and extrapolated from volumes in other Mount Shasta drainages, the predicted planimetric areas subject to lahar inundation from Mud Creek are shown below (Figure 15). These automated DEM-based hazard zone predictions are compared to (1) aerial photography of the 1924 - 1931 Mud Creek lahars, and (2) mapped areas of debris flow hazard by (Osterkamp et al., 1986) based on dendrogeomorphic field evidence (Figure 16).

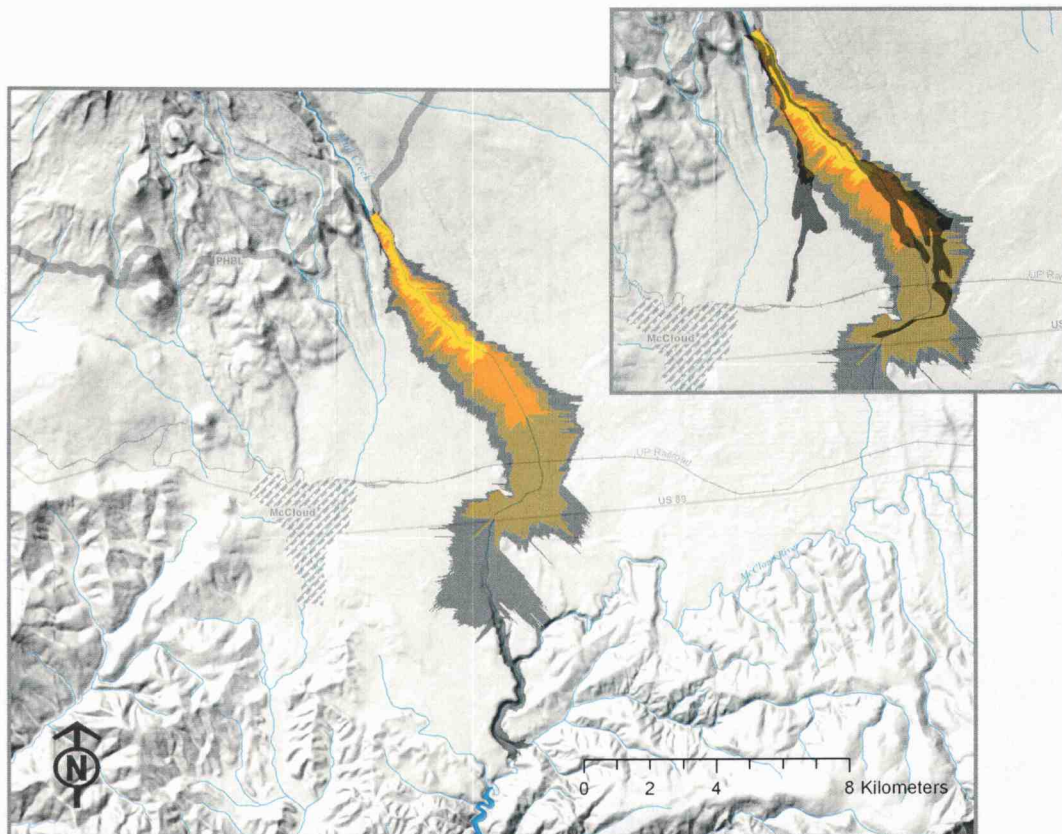


Figure 15 Resulting distal lahar hazard zones for the Mud Creek debris fan. The inset shows an overlay of the approximate area of the 1924 - 1931 Mud Creek debris flows as outlined from a 1944 air photo provided by the USFS McCloud Ranger Station.

Deposition in the Mud Creek basin is shown to begin at a distance of about 10.5 km from the summit and an altitude of 1,480 m, corresponding to the point where the proximal hazard boundary line intersects Mud Creek, below the gorge. This is also the location of the Mud Creek Dam, at the apex of the debris fan as mapped by Miller (1980) and Osterkamp et al. (1986), from which point the 1924 flow and 1925 – 1931 flow series diverge. The largest projected volume (Class 4: $7.0 \times 10^7 \text{ m}^3$) is shown to travel beyond the debris fan into the McCloud River basin, about 32 km from the summit. This scenario would likely generate powerful stream surges that would inundate riparian zones, entrain

additional wood debris and undermine bridges, roads, and reservoirs downstream. The hazard area delineated by Osterkamp et al. (1986) for the Mud Creek Basin is based on geologic and dendrochronologic evidence of at least five lahars in the past 1,200 yr which have covered most of the debris fan including present day McCloud. Changes in microtopography at the apex of the fan could have a significant effect on the path of future lahars over the depositional area.

Table 3. Approximate inundation area and runout distance for modeled lahars from Mud Creek.

Lahar Name		Est. Volume	LZ Area	LZ Distance
Mud 1		$1.5 \times 10^6 \text{ m}^3$	2.64 km^2	17.4 km
Mud 2		$5.0 \times 10^6 \text{ m}^3$	5.85 km^2	19.4 km
Mud 3		$2.3 \times 10^7 \text{ m}^3$	16.18 km^2	24.1 km
Mud 4		$7.0 \times 10^7 \text{ m}^3$	31.24 km^2	31.9 km

In general, the modeled flow of simulated lahars from Mud Creek tends to follow the path of the 1925 – 1931 debris flow series (Figure 15) as well as the high risk area mapped from existing deposits and local topography (Figure 16). The effect of the construction of the Mud Creek Dam in 1925 on the patterns of debris flow travel and deposition is obvious from these results.

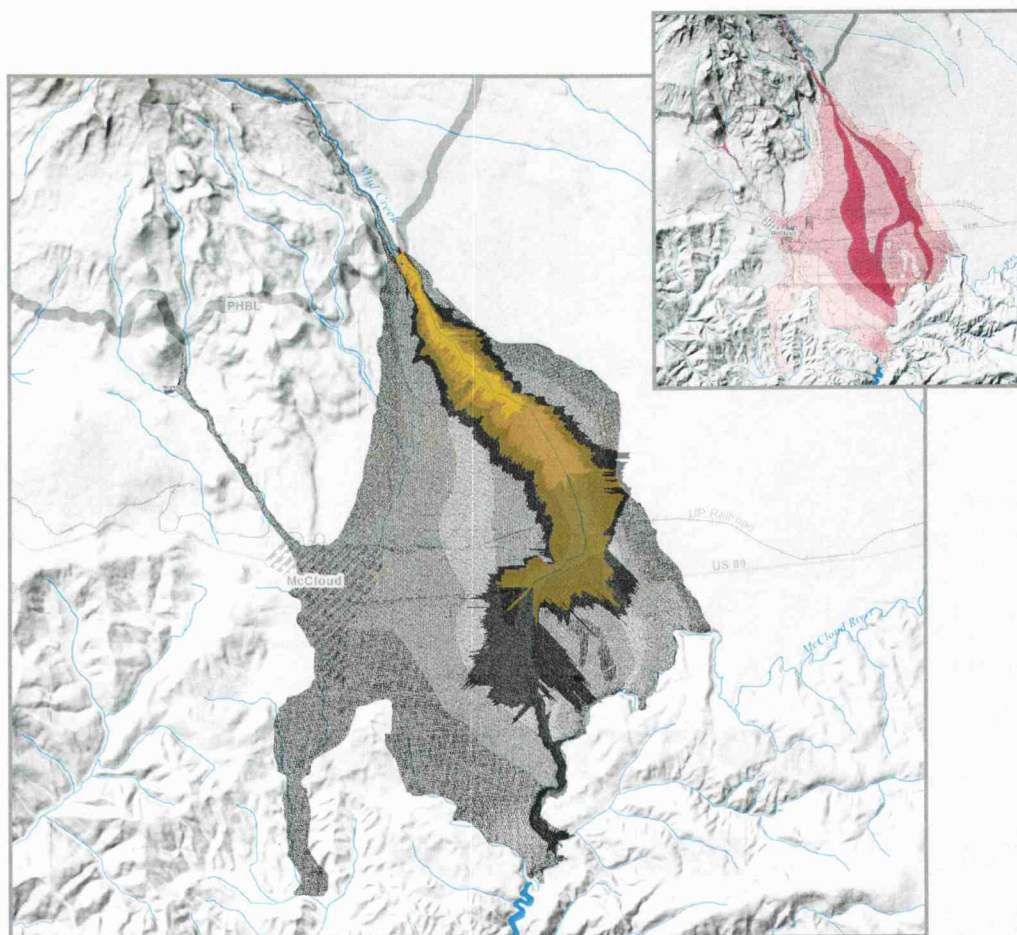


Figure 16 Overlay of the Mud Creek portion of the hazard map by Osterkamp et al., 1986 showing hazard zone gradations related to the probability that a given area will be affected by debris flow activity within the next 100 yr. The high risk areas of most frequent activity are shown in lighter shades and the risk decreases progressively to darker shades.

5. DISCUSSION

Several issues are discussed here that arise in the application of the methodology and the interpretation of results: (1) How severely is the outcome affected by the quality of the DEM?; (2) Is there a rationale for applying the same model parameters to every major drainage on the volcano?; (3) Given the modeling limitations of LAHARZ, how is the

cartographic representation of the generated lahar hazard zones justified?

5.1 DIGITAL TERRAIN AND MODEL LIMITATIONS

5.1.1 IRREGULARITY OF ZONE BOUNDARIES

When comparing mapped patterns of deposition on alluvial fans to inundation areas modeled by LAHARZ, it is apparent that there is more geometrical discrepancy in areas of deposition over broad, flat alluvial fans such as Juniper Flat (Figure 11) than there is on fans with steeper slopes and more pronounced drainage channels, as is the case for Mud Creek (Figure 13). Another feature that is immediately apparent is the irregularity in the "jagged" edges of hazard zones, most clearly seen in Figure 11. This result is due to the construction of a limited number of cross-sections as the program moves downstream cell by cell filling the valley according to equation (1). In areas of irregular topography, a shallow or narrow cross-section will be followed by a deeper and wider one, making the width of the planimetric area irregular. This is also a result of the number of DEM grid cells available and the number of cross-sectional azimuths used by LAHARZ (Figure 17). At certain points, the edge may appear to spike in one direction. This may be indicative of the availability of alternate flow paths in the digital topography. In the case of Whitney Creek, these spikes tend toward areas of known flow diversions.

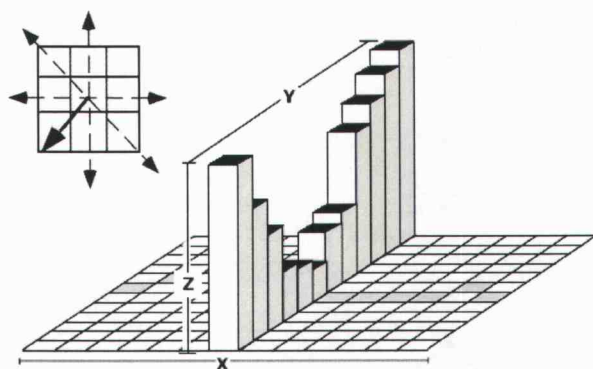


Figure 17 Illustrating the method used by LAHARZ to construct cross-sections, this figure (Schilling, 1998) shows an extruded row of elevation values along the Z axis. Grey cells in the X.Y plane are stream cells. The black tops of the elevated cells form the output planimetric area, once the valley has been filled. The solid arrow (upper left inset) designates the computed flow direction, and the dashed arrows indicate directions of the three computed cross sections.

When comparing real flow diversion to modeled output using LAHARZ, a visualization technique found to be particularly useful is a 3D composite of satellite imagery draped over a DEM showing the georeferenced inundation areas. A perspective view created using ArcScene allows a comparison between irregular hazard boundary lines, the flow path of the 1997 Whitney Creek lahar, and topographic features in the depositional area (Figure 18). From this view, it is clear that parts of the hazard boundary that are stretched out at certain points, correspond to a change in topography that may allow for diversion of the flow.

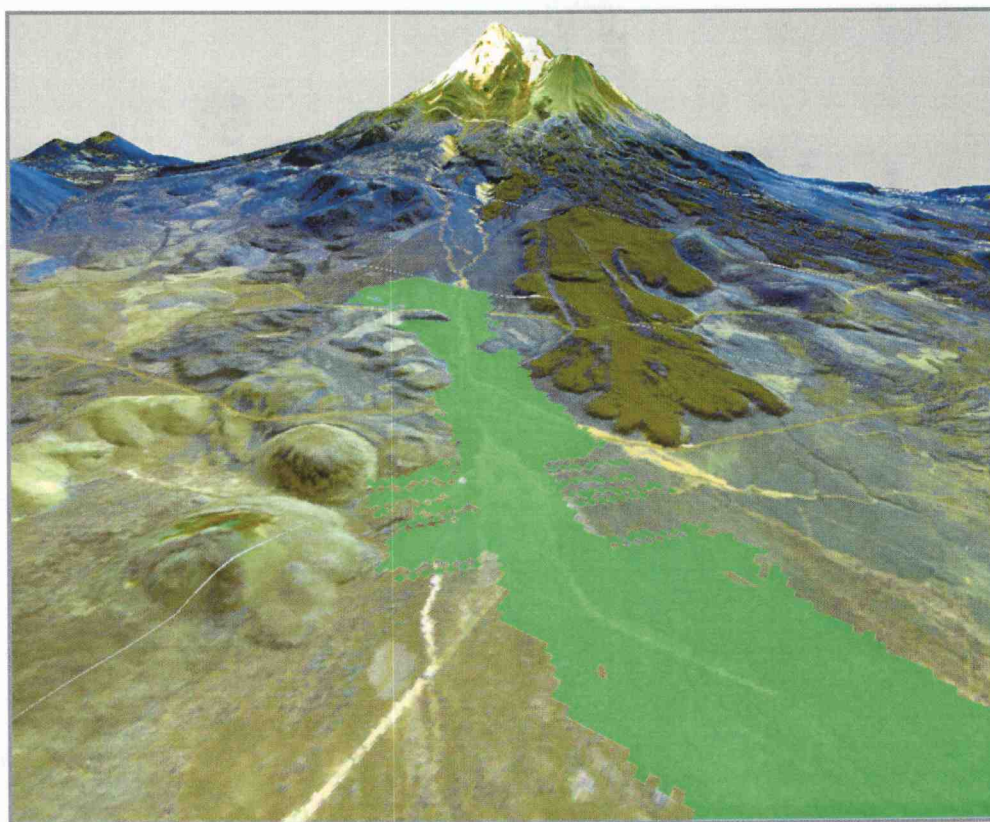


Figure 18 ASTER VNIR composite of bands 1, 2, and 3 show prominent geological features draped over topography. These data are draped over a 10m DEM and adjusted to give a perspective view from the Whitney-Bolam debris fan southeast toward Mount Shasta. The sample lahar inundation area shown in green corresponds to the $5.0 \times 10^6 \text{ m}^3$ flow.

5.1.2 DEM QUALITY AND CULTURAL FEATURES

Another limitation related to the quality of the DEM is the neglect of possible influence by cultural features such as reservoirs and dams. LAHARZ treats all topographic features the same, as stated by Iverson et al. (1998), regardless of what they are. One classic example of this is seen at the head of the Mud Creek debris fan. In 1926, following the flow of 1924 that came close to the town of McCloud and cut off the main water supply (right lobe seen in air photo, Fig 7), a 100-foot long dam was constructed by the McCloud River Lumber Company. It was successful in diverting the first part of the $1.5 \times 10^6 \text{ m}^3$ flow during the summer of 1926, but failed weeks later, allowing a flow 6 m deep to occupy the old channel. The woefully underdesigned dam was reinforced in August, 1926 preceding the flow of 1931, after which diversion projects were revisited in 1935 and 1936 (Hill and Egenhoff, 1976). These structures were apparently large enough to be present in the digital terrain model, as flows simulated were not routed into the old Mud Creek channel of 1924. However, these cultural features are not permanent and their capacity will eventually be exceeded by larger events. The presence of a diversion structure at the apex of the Mud Creek fan throws a wildcard into the equation, elevating the potential for variability in lahar behavior. There are no grounds for claiming that the modeled flow volume of $7.0 \times 10^7 \text{ m}^3$ passing through the dam, will not change course and take the old 1924 channel into McCloud. It is therefore necessary to portray the entire Mud Creek debris fan (Figure 14) as a potential inundation hazard zone, as mapped by Miller (1980) and Osterkamp et al. (1986). In fact, flow diversion on an alluvial fan can be triggered by such commonplace events as a slight breach in the channel wall or confining ridgeline or the displacement of a boulder in the right location. The Whitney Creek flow of 1997 easily found its way around a debris-jammed backwater flow at the U.S. 97 highway culvert, diverting a large part of its volume over the highway a few km to the west (Figs. 5,6).

When mapping lahar hazard zones, it is useful to keep in mind that flow hazards may increase in complexity in drainages headed by dams, much the same way natural dams formed by collapsed canyon walls can result in much more dramatic and unpredictable surges of debris.

Another related limitation is the sensitivity of LAHARZ to subtle variations in digital topography in areas of low relief. If the base DEM does not faithfully represent the true topography, the results can be misleading. As seen in the case of Whitney Creek, an elevated railroad grade or levee on an otherwise smooth surface will influence predicted lahar inundation limits only if the DEM is detailed enough to represent these features. For the 7.5-Minute USGS DEM used here, it is known that 90 percent have a vertical accuracy of 7-m root mean squared error (RMSE) or better and 10 percent are in the 8- to 15-meter range (USGS DEM Fact Sheet 040-00, April 2000). A feature such as the elevated railroad grade which crosses Whitney Creek below the confluence with Bolam and Graham Creeks, can easily go unnoticed. This seems to be the case of the result for predicted areas below this point. When modeling the flow of small lahars, if 30 m is a significant fraction of the inundated valley width in depositional areas, then a DEM of greater resolution will produce more meaningful results. The same would be true if it were critical to detect subtle variations in the microtopography of a debris fan. However, as the flow volume gets larger, there is less influence on flow direction and planimetric deposition area by these features.

5.1.3 OTHER LIMITATIONS

LAHARZ does not predict overbank flow or stream diversion. It also does not account for changes in rheology from cohesive or non-cohesive lahar to hyperconcentrated flow to

regular streamflow. The effects of bulking, grain size, and frictional coefficients that regulate flow behavior are not modeled. Despite this long list of limitations, LAHARZ is successful in its attempt to predict general flow path and downstream inundation area in a way that responds to variations in topography and flow volume. LAHARZ assumes that deposition begins at the PHZB line and therefore, the effects of bulking from the source to the beginning of the distal zone are considered accounted for in the design volume used. It is hence not advisable to blindly model inundation based on an "input hydrograph" from volumes of available water equivalent or debris in initiation areas.

5.2 PREDICTED VOLUMES AND SOURCES OF LAHARS

The volumes chosen for the purpose of mapping consistent categories of lahar hazards for Mud and Whitney Creek basins were based on four scenarios involving triggering mechanisms known to operate on Mount Shasta. The volumes represent four size classes of lahars ranging in frequency/impact relationship from high/low to low/high. Although our records of event frequency relative to volume may be skewed by the tendency to identify the most recent flow deposits in the field (Osterkamp et al., 1986), there are several frequency/size indicators which may provide a basis from which to predict which volumes and trigger mechanisms are most likely for future lahars at Mount Shasta.

One such indicator is debris flow frequency in relation to channel incision. Figure 19, from Osterkamp et al. (1986), shows a linear relationship between gorge depths and known flow frequency during the last 500 yr for drainage basins of Mount Shasta. The data suggest a strong relationship between debris flow frequency and incision depth ($r = 0.91$). Osterkamp et al. (1986) take this as evidence that the main sediment source areas are the unvegetated valley walls within the gorges.

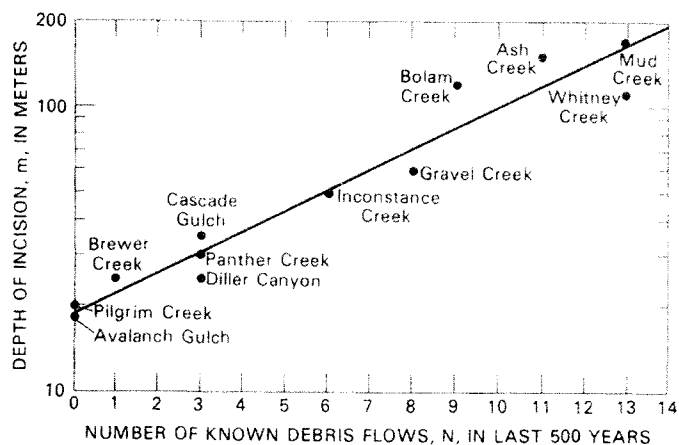


Figure 19 Modified from Osterkamp et al. (1986), this graph relates the depths of stream channel incisions on Mount Shasta to the known number of debris flows from each stream in the past 500 yr.

Large magnitude flows, syneruptive or not, will need to mobilize large amounts of unconsolidated pyroclastic debris in the proximal zone. Mud and Whitney Creek gorges appear to be the greatest sources for bulking lahars. The extrapolation of the same high flow volumes to drainages where channel failure is not likely due to the absence of steep erodible pyroclastics, may not be the best approach. Some scaling may be required based on available water and debris sources. Even in channels not headed by glaciers, massive syneruptive flows may be possible during times of heavy snowpack if the local source for debris exists.

Another consideration in the prediction of future lahar volumes of noneruptive origin may be climate change. Debris flow activity during recent centuries may have been more intense than it was during earlier parts of the Holocene time (Osterkamp et al., 1986). According to Rhodes (1987), Mount Shasta was experiencing drought conditions between 1917 and 1936, with an estimated loss of half the ice volume on the stratovolcano. Interestingly, in the last several years, higher amounts of precipitation at Mount Shasta have resulted in the renewed growth of its glaciers (McFarling, 2003), despite overall warmer temperatures. This trend of prolonged drought and hot summers following periods

of glacial growth appears to have contributed to the destabilization of the Konwakion glacier. On the opposite side of the mountain, flows have typically been triggered by warm, heavy rainfall events over glaciers where the preceding winter snowpack was light (Callaghan, 2000). Several other converging events, such as snowmelt, glacial outburst floods, slope failures by water saturation, and channel damming and breakthrough seem to have contributed to the generation of the largest Whitney Creek flows.

The largest category of lahar envisioned in this study could potentially occur on any side of Mount Shasta if a considerable water source (either snowpack or glacial ice) were to liquefy debris in a flank collapse or debris avalanche. Studies have shown that steep areas of hydrothermal alteration (a usual indicator of collapse potential) on the flanks of Mount Shasta are not as prevalent as they are on Mount Adams and Mount Rainier (Crowley et al., 2003). However, hydrothermal systems are present and active on Mount Shasta (Hirt, 2000) and water-saturated areas could fail along with large volumes of glacial ice, especially if earthquakes, magmatic intrusion, or eruption is involved (Scott et al., 2001).

5.3 LAHAR HAZARD ZONES AND MAPPING CONSIDERATIONS

The four overlapping hazard zones shown for Mud and Whitney Creek basins are color-coded by volume potential. Although most mapped lahar hazards using LAHARZ are qualitatively ranked from high to low, probable recurrence intervals can be assigned to lahars for a more quantitative interpretation. However, this could be misleading to those who are not familiar with hazard recurrence intervals, giving the impression that a 500-year flood cannot occur sooner than a 100-year flood.

The hazard zones shown here were left unedited, but some smoothing of the jagged edges may be necessary to communicate that there is a lot of potential variability in the extent of inundation areas and that the areas delineated are not to be taken as absolute hazard boundaries. As mentioned above, lahar behavior is much less predictable than portrayed on a hazard map like the one featured here. Changes in topography due to deposition and erosion by frequent flows and other processes such as natural damming in stream channels can quickly change the topography and significantly alter the flow path. Although in no immediate danger, inhabitants of towns such as McCloud and Mount Shasta City partially situated on a debris fan, and communities such as Dunsmuir downstream from active drainages, should be aware of the fact that inundation is possible over any part of the fan. Just as important as visually communicating hazard potential and variability in a geographic context is Education for Self Warning and Evacuation (Scott et al., 2001). A simple visual message posted at campgrounds and trailheads in Mount Rainier National Park, Washington (Figure 20) reminds people in flow pathways to go to high ground immediately following any ground tremor or any prolonged

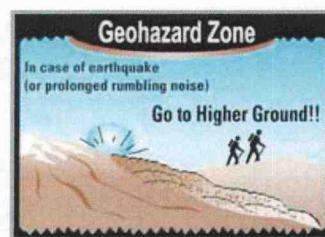


Figure 20 From Scott et al (2001) this warning sign (above) is posted at campgrounds and trailheads in Mount Rainier, Washington. The trailhead sign shown on the left was buried by the 1997 Whitney Creek lahar. This flow size class occurs with a frequency of at least once per decade.

rumbling noise from upstream. Simply walking about 75 m uphill from their homes would have saved most of the 23,000 people who died from lahar inundation at Nevado del Ruiz, Colombia in 1985 (Scott et al., 2001). Ultimately, the greatest value of a well-designed cartographic product outlining areas most vulnerable to lahar inundation downstream from a volcano is its ability to communicate the information necessary to prevent loss of life and property.

6. CONCLUSIONS

In this thesis, a lahar-hazard zonation map was constructed for the Mud and Whitney Creek drainages of Mount Shasta using a 30-m resolution DEM, potential event volumes based on the geologic record, and the LAHARZ inundation modeling tool.

Based on field evidence from historic lahars of Whitney Creek (1935, 1985, 1997) and Mud Creek (1924 – 1931), as well as the late Pleistocene Big Canyon Creek lahar, four magnitude classes of lahars were selected: (1) 1.5×10^6 , (2) 5.0×10^6 , (3) 2.3×10^7 , and (4) 7.0×10^7 m³. Classes 1 – 3 have been generated on Mount Shasta in association with climatically induced glacier outburst floods, ice avalanching, intense convective precipitation events, failure of channel walls, and/or breaching of natural debris dams. The largest category used, 7.0×10^7 m³, is derived from the evidence of the Big Canyon Creek lahar, which is likely to have formed at the time of the gigantic debris avalanche from the collapse of ancestral Mount Shasta. This size class is considered possible in association with eruptive activity (hot pyroclastic material melting snow and ice), or flank collapse scenarios. Although the generation of this category of lahar is not an immediate

possibility, and has not occurred since the late Pleistocene, the eruptive frequency of Mount Shasta and its history of flank collapse, as well as the evidence of the Big Canyon Creek lahar underlying parts of present day Mount Shasta City suggests that a lahar of this magnitude will eventually occur.

Based on modeling over the topography of Mud and Whitney Creek basins, the depositional areas of class 1 and class 2 lahars are likely to be confined to the debris fan, reaching up to 9 km from the PHZB (Tables 2 and 3). Class 3 lahars are predicted to have sufficient volume to reach Lake Shastina (12.8 km from the PHZB) from Whitney Creek and Highway 89 or McCloud (13.6 km from the PHBZ) from Mud Creek. The farthest-reaching hazard zone in the distal area is for class 4 lahars. The predicted runout distance of these lahars (about 21 km from the PHBZ) is a threat to immediate infrastructure (Union Pacific Railroad, Highways 89 and 97, McCloud, and I-5) as well as a hazard to communities that would be affected by the severe disruption of the McCloud River and Shastina Lake.

The hazard zones resulting from the LAHARZ-predicted inundation areas are color-coded according to potential volume. Further development of this map (Appendix E) could represent some of the variability in potential flow paths (discussed above, Section 5.1.2) by outlining the parts of the debris fan that have been affected by lahars in the past. A gradation of lahar hazard from "high" to "low" is also helpful, assuming adequate explanation of this range is provided.

The following conclusions were made based on the results of the study:

- 1) Cultural features can have a significant effect on the behavior of a lahar, especially when located at the head of a debris fan, where flowing debris is more sensitive to minor changes in topography. A diversion dam located at the head of the Mud Creek debris fan

and a railroad grade and culvert at the head of the Whitney Creek debris fan are examples of the importance of obtaining a DEM of sufficient quality before producing LAHARZ hazard maps.

2) In the development of lahar inundation hazard maps using LAHARZ, the energy cone ration (H/L) value may need to be calibrated to the topography of each individual drainage, depending on the size of the lahar being simulated and its expected runout distance. A proximal hazard boundary line drawn close to the volcano, as is the case for Mount Shasta (H/L = 0.266) assumes most of the volume will be deposited near volcano flanks. The opposite is true for volcanoes such as Mount Rainier, where large flow volumes and extended channel systems are able to transport debris far from volcano flanks (H/L = 0.23). Calibration of this value should be based on field data.

3) The Big Canyon Creek Lahar which occurred on the South flank of Mount Shasta (possibly in conjunction with the giant debris avalanche to the northwest) is likely to have traveled a greater distance than it would have had it occurred in the Mud or Whitney Creek drainages. Its estimated volume of $7.0 \times 10^7 \text{ m}^3$ was probably quickly re-channelized into the Sacramento River valley as it devastated the area which is now occupied by Dunsmuir (Figure 11). A similar event, although highly unlikely in the near future, would have serious impacts on communities downstream from Mount Shasta's inundated watersheds.

4) The limitations in the methodology discussed above translate into a degree of uncertainty in regard to mapped limits of distal hazard zones that must be communicated to the viewers. The following caption included in the hazard map is considered an appropriate and necessary disclaimer:

"NOTE: This map contains sharp boundaries for all hazard zones. The degree of hazard does not change abruptly at these boundaries. Rather, the hazard decreases gradually as distance from the volcano increases and areas immediately adjacent to hazard zone boundaries should not be regarded as hazard free. These boundaries are located only approximately, as a degree of uncertainty exists regarding the source, size and mobility of future lahars. It should be noted, however, that hazard decreases rapidly as elevation above the valley floor increases."

7. REFERENCES

- Blodgett J C, Poeschel K R, and Osterkamp W R (1996). *Characteristics of Debris Flows of Noneruptive Origin on Mount Shasta, Northern California*. U.S. Geological Survey Open-File Report 96-144. Sacramento, California.
- Callaghan, C J (2000). *Debris Flow Initiation Conditions on Mount Shasta, California*. MS Thesis: Geological Engineering, University of Nevada, Reno.
- Capra L, Poblete M A, Alvarado R (2004). The 1997 and 2001 lahars of Popocatepetl volcano (Central Mexico): textural and sedimentological constraints on their origin and hazards. *Journal of Volcanology and Geothermal Research*, 131, no.3-4 (30 MAR 2004) p. 351-369.
- Crandell, D R (1971). *Postglacial Hazards from Mount Rainier Volcano, Washington*. USGS Professional Paper 677 (1971) 75p.
- Crandell D and Nichols D (1987). *Volcanic Hazards at Mount Shasta, California*. Washington, D.C.: U.S. Geological Survey, Department of the Interior, 1987. Pamphlet.
- Crandell D R (1989). *Gigantic debris avalanche of Pleistocene age from ancestral Mount Shasta Volcano, California, and debris-avalanche hazard zonation*. U.S. Geological Survey Bulletin 1861, 32 p.
- Crowley J K, Hubbard B E and Mars J C (2003). Analysis of potential debris flow source areas on Mount Shasta, California, by using airborne and satellite remote sensing data. *Remote Sensing of the Environment*, 87 (2003) 345-358.
- De la Fuente J and Bachmann S (1998). *The Whitney Creek Debris Flow of August 20, 1997: Triggering Mechanism, Processes, and Sources of Debris*. U.S. Forest Service Report.
- Dickson B A and Crocker R L (1953). A chronosequence of soils and vegetation near Mount Shasta, California, part I: Definition of ecosystems investigated and features of plant Succession. *Journal of Soil Science*, Vol. 4, No. 2, p 123-141.
- Driedger C L and Kennard P M (1986). *Ice Volumes on Cascade Volcanoes: Mount Rainier, Mount Hood, Three Sisters and Mount Shasta*. US Geological Survey Professional Paper 1365 (1986) 28p.
- Hayashi J N and Self S (1992). A comparison of Pyroclastic Flow and Debris Avalanche Mobility. *Journal of Geophysical Research*, Vol. 97, no. B6, p. 9063-9071.
- Hill M and Egenhoff E L (1976). A California jökulhlaup. *California Geology*, v. 29, no. 7, p. 154-158.

- Hirt W H (2004). *An Overview of the Geology of Mount Shasta*. Weed, CA: College of the Siskiyou, Division of Natural and Applied Sciences.
- Hupp C R, Osterkamp W R and Thornton J L (1987). *Dendrogeomorphic Evidence and Dating of Recent Debris Flows on Mount Shasta, Northern California*. U.S. Geological Survey Professional Paper 1396-B.
- Iverson R M, Schilling S P and Vallance J W (1998). *Objective Delineation of Lahar-inundation Hazard Zones*. Geological Society of America Bulletin, v. 110, p. 972-984.
- Malin M C and Sheridan M F (1982). Computer-assisted mapping of pyroclastic surges. *Science* 217, 637-639.
- McCloud Fly Fishing Club (2001) *The Mount Shasta Companion Historic Mud Creek Photo Collection: September 1924 Annotated Photo Album of Mud Creek Debris Flow*. Retrieved March 10, 2004 from the World Wide Web: <http://www.siskiyou.edu/shasta/env/mudflow/index.htm>
- McFarling U L (2003). *Survey Finds Sierra Nevada Glaciers are in Rapid Retreat*. Los Angeles Times, October 12, 2003.
- Miller C D (1980). *Potential Hazards from Future Eruptions in the Vicinity of Mount Shasta Volcano, Northern California*. USGS Bulletin 1503. Washington, D.C.: United States Government Printing Office, 1980.
- Monmonier M (1997). *Cartographies of Danger: Mapping Hazards in America*. London: University of Chicago Press, Ltd. 363 p.
- Mothes P A, Hall M L and Janda R J (1998). *The enormous Chillos Valley Lahar: an ash-flow-generated debris flow from Cotopaxi Volcano, Ecuador*. Bulletin of Volcanology (1998) 59:233-244.
- Osterkamp W R, Hupp C R and Blodgett J C (1986). *Magnitude and frequency of Debris Flows, and Areas of Hazard on Mount Shasta, Northern California*. U.S. Geological Survey Professional Paper 1396-C. 1986. p. C1-C21.
- Pierson T C and Scott K M (1985). Downstream Dilution of a Lahar: Transition from Debris Flow to Hyperconcentrated Streamflow, *Water Resources Research*, v.21, No. 10, p 1511-1524, October 1985.
- Pierson T C, Janda R J, Thouret J, and Borrero, C A (1990). Perturbation and melting of snow and ice by the 13 November 1985 eruption of Nevado del Ruiz, Colombia, and consequent mobilization, flow and deposition of lahars. *Journal of Volcanology and Geothermal Research*, 41 (1990) 17-66.
- Rhodes P T (1987). Historic glacier fluctuations at Mount Shasta, Siskiyou County: *California Geology*, v. 40, p. 205-209.

- Roberts, M (2004). *Pleistocene and late holocene lahars from the southern flank of Mount Shasta, California; characteristics and hazard implications*. MS thesis, Humboldt State University.
- Schilling S P (1998). *LAHARZ: GIS programs for automated mapping of lahar-inundation zones*. U.S. Geological Survey Open-File Report, 98-638.
- Scott K M, Vallance J W, and Pringle P T (1995). *Sedimentology, Behavior, and Hazards of Debris Flows at Mount Rainier, Washington*. U.S. Geological Survey Professional Paper 1547, 56 p.
- Scott K M, Macias J L, Naranjo J A, Rodriguez S and McGeehin J P (2001). *Catastrophic Debris Flows Transformed from Landslides in Volcanic Terrains: Mobility, Hazard Assessment, and Mitigation Strategies*. U.S. Geological Survey Professional Paper 1630. 59 p.
- Sisson J H (1884). Local Indian Names around Mount Shasta, California. [Abstract of Notebook Containing Vocabularies and other Linguistic Notes on a Variety of American Indian Languages. In: Miesse, W.C. (1993) *Mount Shasta: An Annotated Bibliography*. Weed, California: College of the Siskiyous. viii, 289 p.
- The Mount Shasta Companion (2001) *Environmental Setting: Weather and Climate: The Glacial History of Mount Shasta: Mudflows*. Retrieved March 10, 2004 from the World Wide Web: <http://www.siskiyous.edu/shasta/env/glacial/mud.htm>
- UCSB Press Release (2005) *Small Glaciers in Northern California Buck Global Warming Trend*. May 5, 2005. Santa Barbara, CA. Retrieved May 14, 2005 from the World Wide Web: <http://www.ia.ucsb.edu/pa/display.aspx?pk=1288>
- USGS (2000) DEM Fact Sheet 040-00: *US GeoData Digital Elevation Models*. April 2000. Retrieved May 20, 2005 from the World Wide Web: <http://mac.usgs.gov/isb/pubs/factsheets/fs04000.html>
- Vallance J W and Scott K M (1997). *The Osceola Mudflow from Mount Rainier; Sedimentology and hazard implications of a huge clay-rich debris flow*. Geological Society of America Bulletin v.109 no. 2, p.143-163.
- Zanger M (1992). *Mt. Shasta: History, Legend & Lore*. Berkeley, California: Celestial Arts, 120 p.

APPENDIX A

HISTORIC PHOTOS OF THE 1924 MUD CREEK LAHAR

This set of historic photos is part of the Mount Shasta Collection available at the College of the Siskiyou Library in Weed, California. The collection, established and developed by Dennis Freeman and Bill Miesse is the largest repository of information and documents about Mount Shasta. The collection consists of thousands of books, articles, manuscripts, photographs, maps, prints, and audiovisual materials about the Mount Shasta volcano and surrounding area. The photos shown here were made available online courtesy of the McCloud Fly Fishing Club at <http://www.siskiyou.edu/shasta/env/mudflow/>. The album is copyrighted (1924) by Morton & Co. of San Francisco. It shows photographs of the 1924 Mud Creek debris flow with original annotations. At the time, Mount Shasta City had the name Sisson, after Justin Hinckley Sisson, who arrived in 1853 and established the town. This photo collection is a good primary source for reconstructing the series of events which led to the mudflows of 1924 near McCloud, California.

APPENDIX A: HISTORIC PHOTOS OF THE 1924 MUD CREEK LAHAR

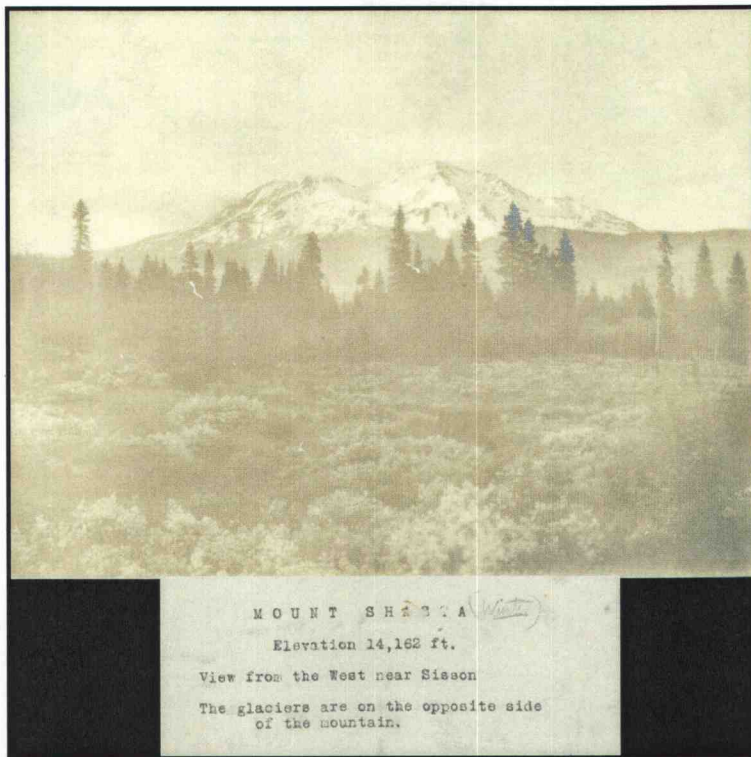


Photo 1: Mount Shasta from Sisson

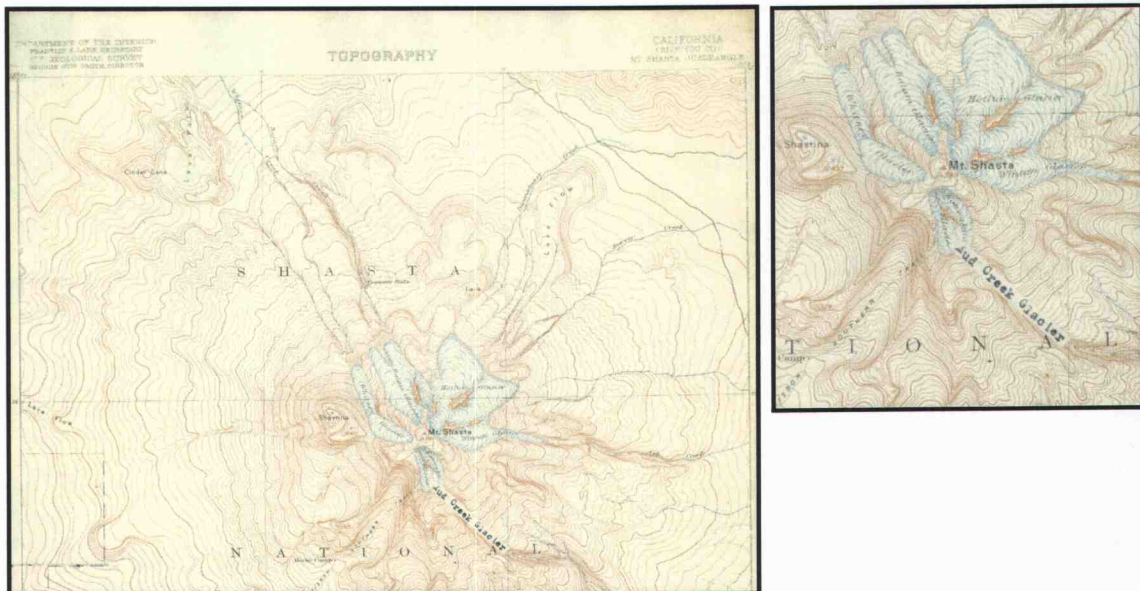


Photo 2: Mount Shasta Topographic Map with glaciers close-up

Mount Shasta's summit is 14,162 feet above the sea but from about the 12,000' level the terrain is covered with perpetual snow and rock and circled by five large glaciers which are situated by the points of the compass from the summit rocks as follows:-

North slope	Hotlum and Bolam Glaciers
East slope	Wintoon glacier
West slope	Whitney glacier
South slope	Konwakiton glacier

This last named is popularly known as Mud Creek or Mc Cloud glacier as it is the source of the Mc Cloud River.

In ordinary years the winter snow is not melted off these ice fields until about July and then the glaciers commence to melt and discharge their milky white water into the streams which flow from the mountain.

Whitney and Bolam creeks sink out of sight at about the 4000 the foot level and only streams which reach the foot of the mountain are Ash and Mud Creeks which form the head waters of the Mc Cloud River. The former (Ash Creek) also is the water supply of the town of Mc Cloud.

Last winter 1924 by reason of the light snow fall the glaciers were free of snow by the first of May and commence to melt and discharge large streams of water. These meltings being principally along the sides the water ran under the ice and soon formed channels and so undermined the foundations so that after two months of melting; particularly the Mud Creek Glacier; by the end of June the bodies of ice commenced to break off at the lower ends and falling some hundreds of feet carried great masses of rock sand and gravel with them.

Observers stated that with sounds like the discharge of cannon masses as large as an ordinary house would break off every two or three minutes and away they would go down the canyon. The resultant avalanches wrecked the Mc Cloud water works, carried out the camp of the water tenders, made a great slope of glacial sand some seven miles long and a mile or more wide, with a depth of from five to thirteen feet and discolored the Mc Cloud, the Pit and the Sacramento Rivers for miles from ~~the~~ source.

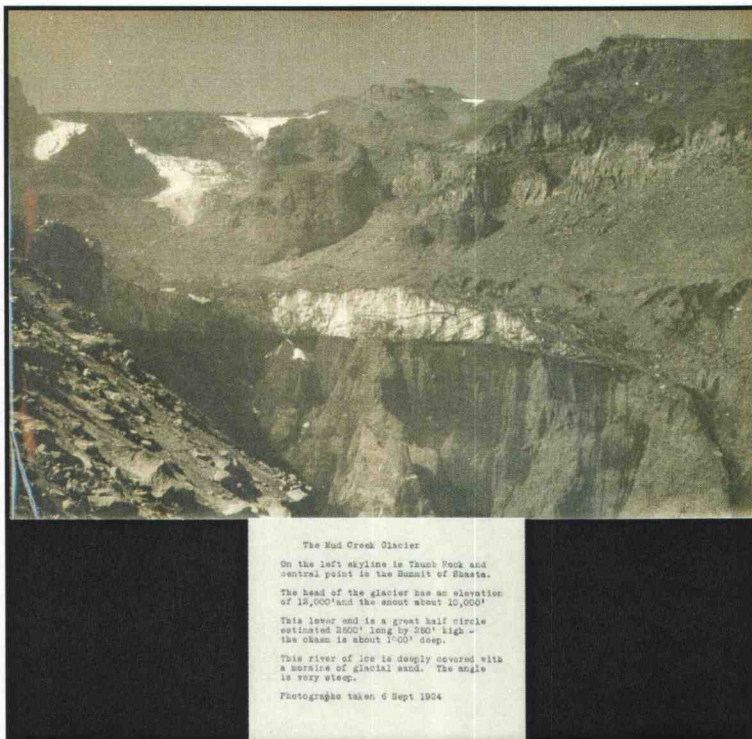
San Francisco 12 September 1924

Photo 3: Introduction

Observers stated that with sounds like the discharge of cannon masses as large as an ordinary house would break off every two or three minutes and away they would go down the canyon. The resultant avalanches wrecked the Mc Cloud water works, carried out the camp of the water tenders, made a great slope of glacial sand some seven miles long and a mile or more wide, with a depth of from five to thirteen feet and discolored the Mc Cloud, the Pit and the Sacramento Rivers for miles from ~~the~~ source.

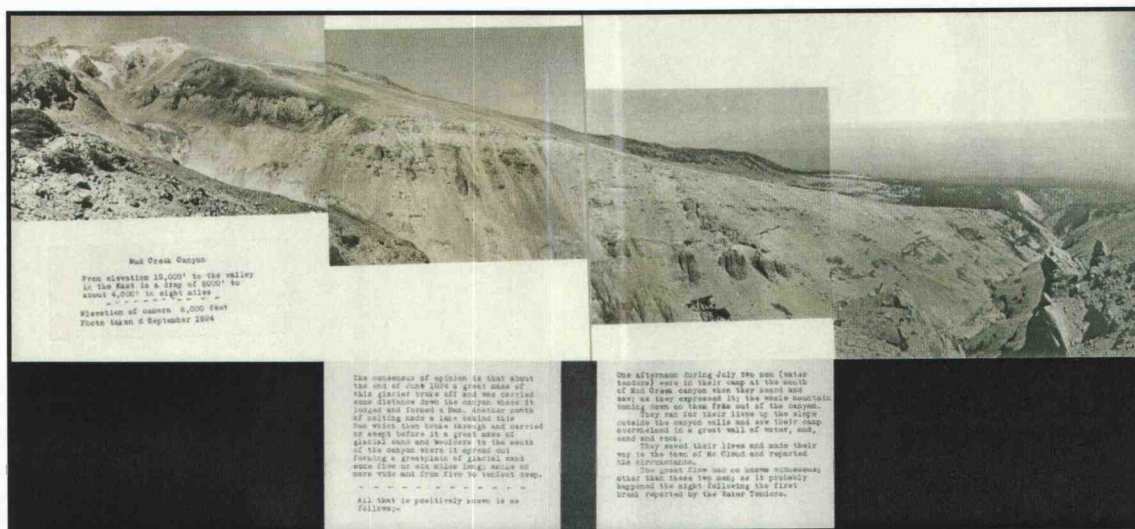
San Francisco 12 September 1924

Photo 4: Introduction, part 2



The Mud Creek Glacier
 On the left skyline is Thumb Peak and central point is the Summit of Shasta.
 The head of the glacier has an elevation of 12,000' and the snout about 10,000'.
 This lower end is a great half circle estimated 2500' long by 250' high - the cham is about 1'-00' deep.
 This river of ice is deeply covered with a surface of glacial sand. The angle is very steep.
 Photographs taken 6 Sept 1904

Photo 5: Overhanging Mud Creek Glacier Terminus



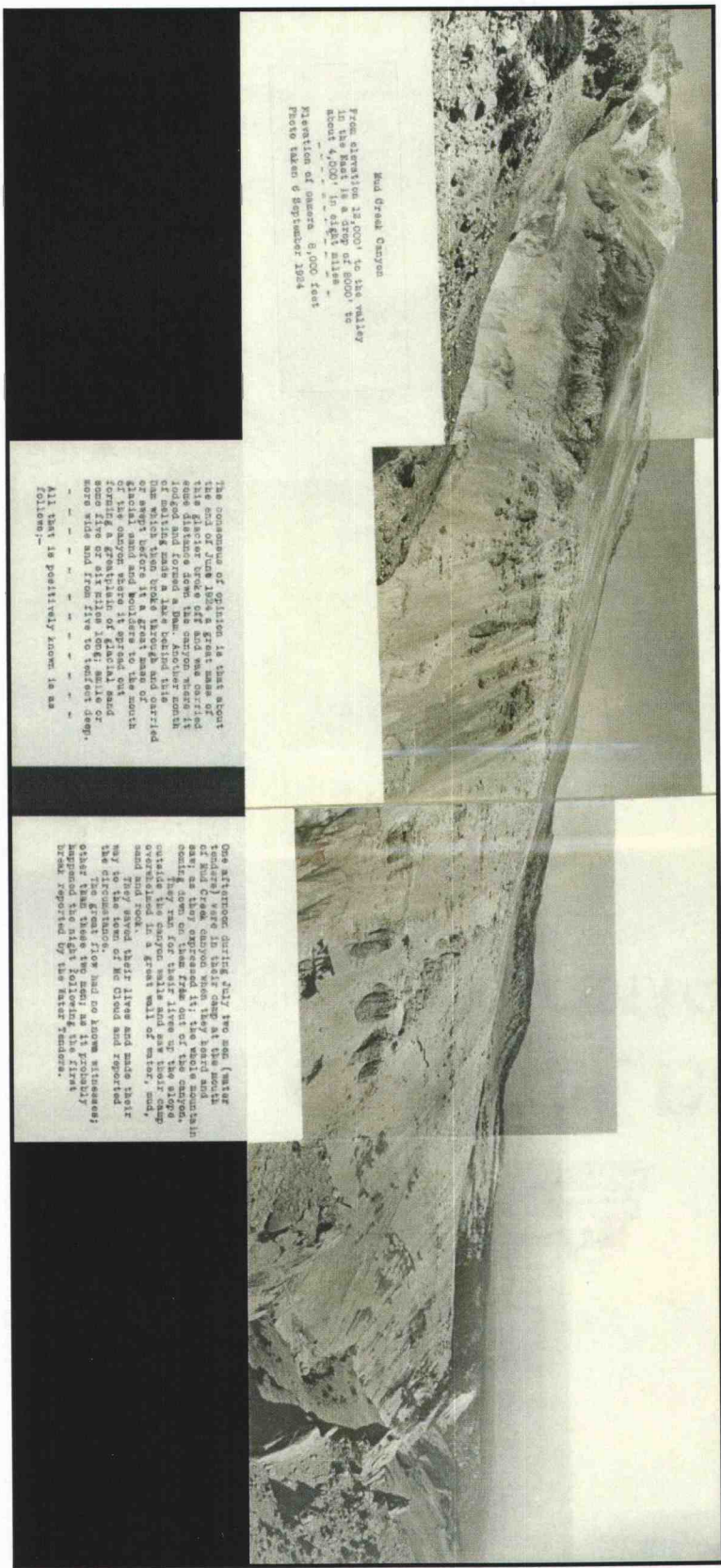
Mud Creek Canyon
 From elevation 10,000' to the valley in the East is a line of 6000' to about 4,000' in eight miles.
 Elevation of camera 8,000 feet
 Photo taken 6 September 1904

The consensus of opinion is that about the end of June 1904 a great mass of this glacier broke off and was carried some distance down the canyon where it lodged and formed a Dam. Another month of melting sand & ice behind this Dam which then broke through and carried off great sections of a great mass of glacial sand and boulders to the south of the canyon where it formed out forming a great plain of glacial sand some five or six miles long. Much of this was the Mud Creek flow to which I refer.

One afternoon during July 1904 men (water hauled) were in their camp at the mouth of Mud Creek canyon when they heard and saw as they approached in the same direction coming down on them from out of the canyon. They ran for their lives up the slope outside the canyon walls and saw their camp surrounded in a great wall of water, mud, sand and rock.
 They saved their lives and made their way to the town of Mc Cloud and reported the circumstances.
 The great flow had no other consequences other than these two and, as it probably happened the night following the first event reported by the latter travelers.

All that is positively known is as follows:

Photo 6: Panorama of debris source area: Mud Creek Canyon



Mud Creek Canyon
 From altitude 12,000' to the valley
 is the East is a drop of 8000' to
 about 4,000' in eight miles -
 Elevation of mesa 8,000 feet
 Photo taken 6 September 1964

The maximum of glacial ice about
 the end of June 1964 a great mass of
 this glacier broke off and was carried
 down the canyon. The ice then melted
 and formed a lake between the mouth
 of melting water a lake behind the
 rim which then broke through and carried
 down the canyon where it spread out
 forming a great plain of glacial sand
 and gravel. The ice then melted and
 glacial sand and boulders to the south
 of the canyon where it spread out
 more wide and from give to "red dirt" deep.

On afternoon during July two men (water
 tender) were in their camp at the mouth
 of the canyon. They were looking at the
 sand as they expressed it; the whole mountain
 side on the fire out of the canyon.
 They ran on their feet and the ridge
 overland in a great wall of water, sand
 and rock. They then left and made their
 way to the town of Mt. Hood and reported
 the circumstance.
 The Great Fire had no known witnesses;
 other than the fact that the fire
 happened the night following the first
 break reported by the water tender.

Photo 6a (enlarged): Panorama of debris source area: Mud Creek Canyon

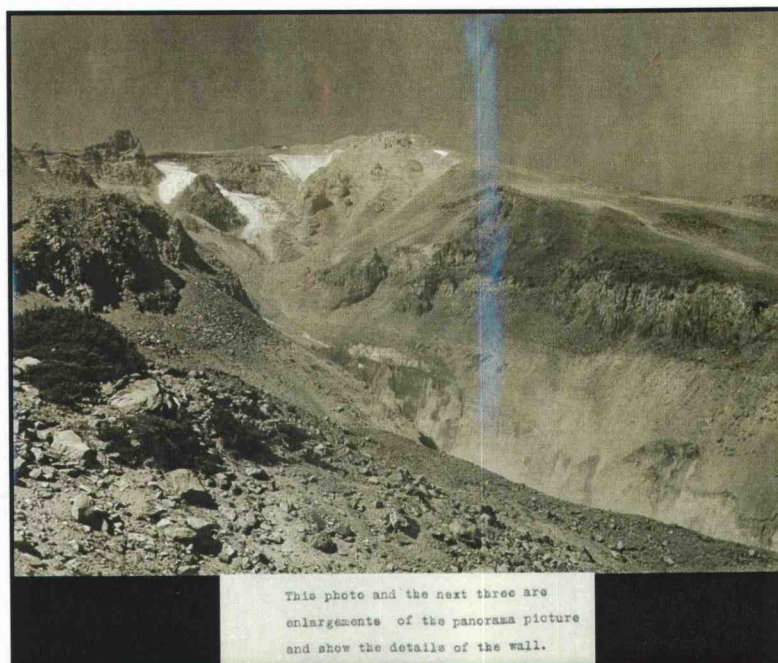


Photo 7: Part 1 of Mud Creek Canyon



Photo 8: Part 2 of Mud Creek Canyon

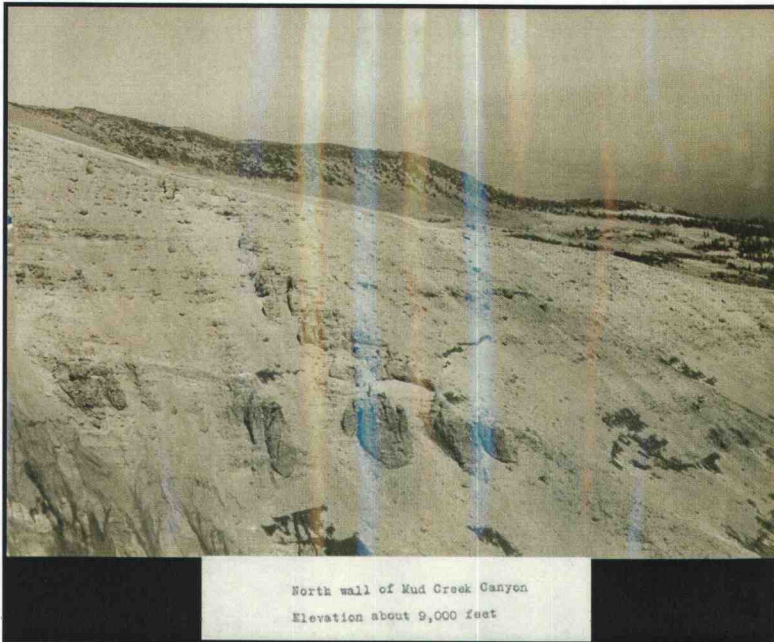


Photo 9: Part 3 of Mud Creek Canyon

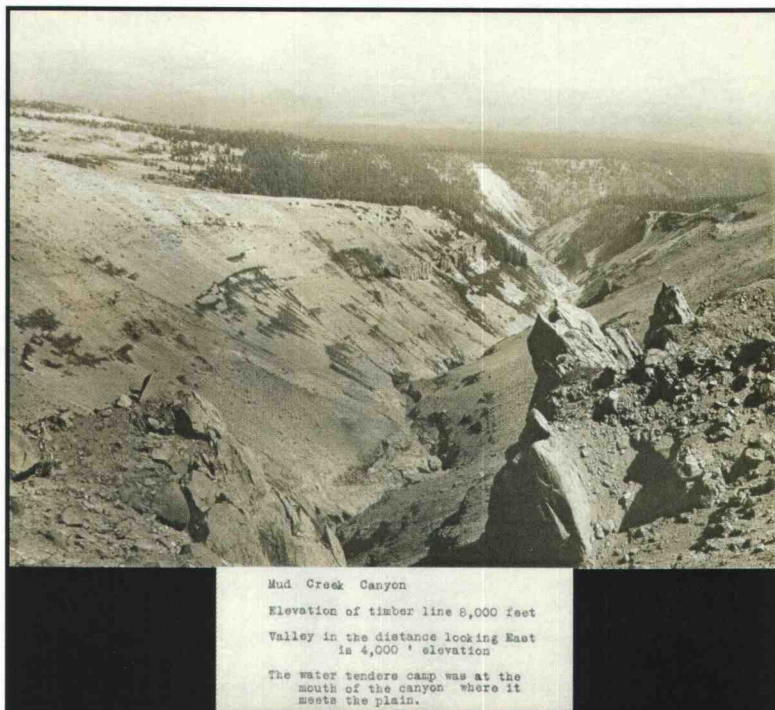


Photo 10: Part 4 of Mud Creek Canyon

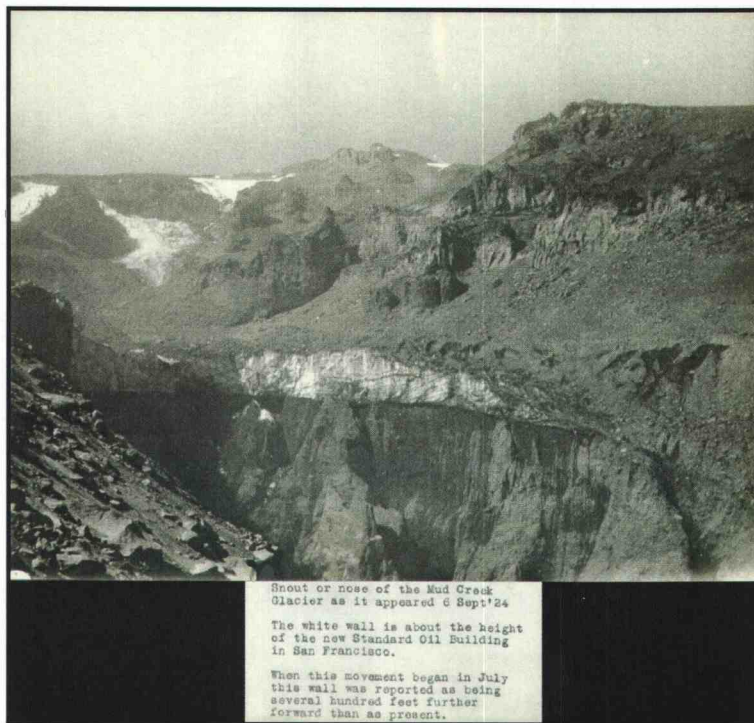


Photo 11: Terminus of the Mud Creek Glacier

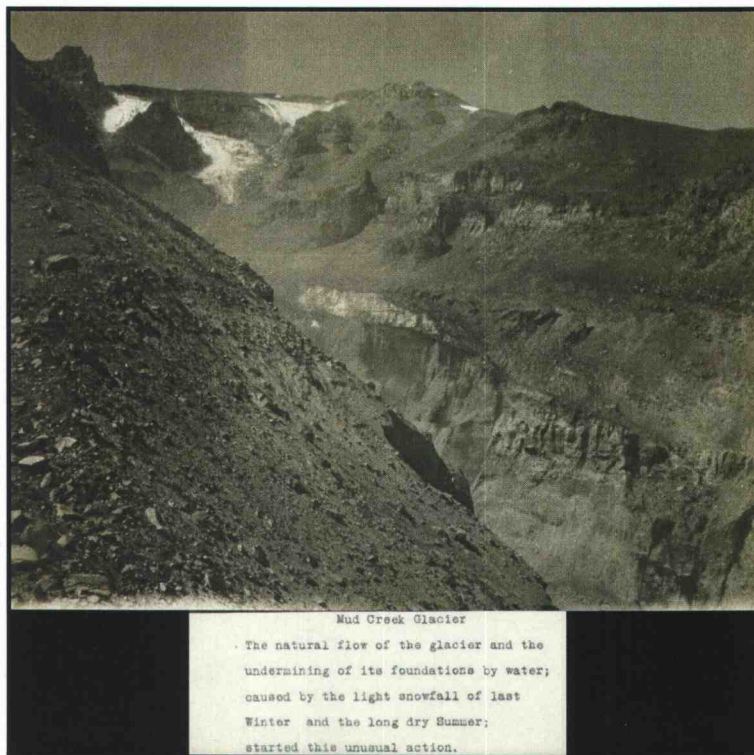
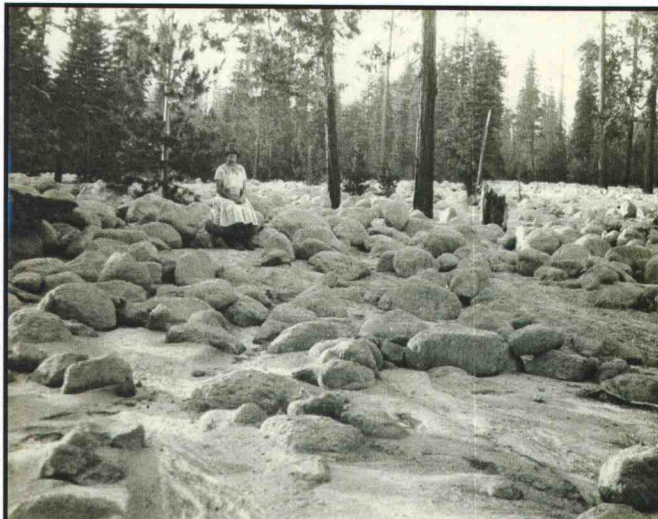


Photo 12: The Mud Creek Glacier from below the canyon wall



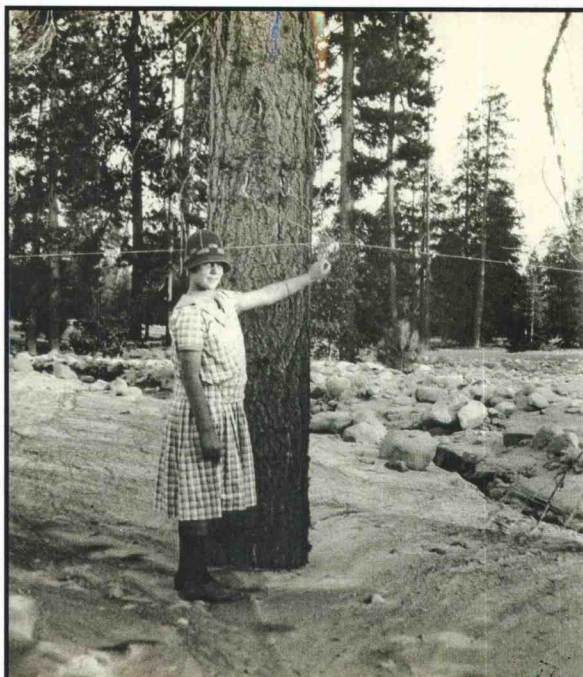
Great Field of Glacial Boulders

These rocks, the size of a trunk, were carried along in the flood of water and sand like so many pebbles.

Showing the powerful hydraulic force caused by the weight of water and sand coming from a great elevation.

Photograph taken 8 Sept 1924

Photo 13: Field of boulders left along Mud Creek



The flow is thirteen feet deep at this point.

This standard telegraph wire was erected 18' above the forest floor, and is now but five feet above the glacial deposit.

Photo 14: Indicators of the flow depth

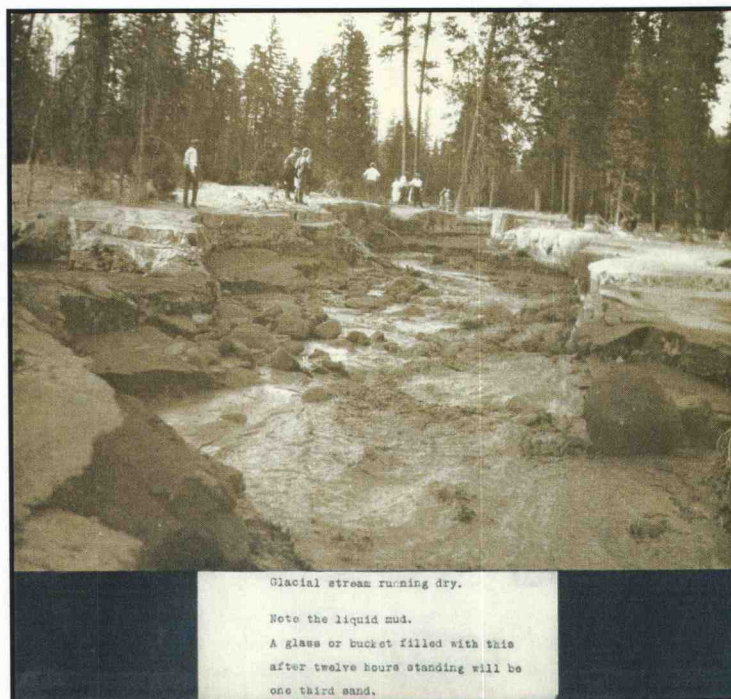


Photo 15: Aftermath of the debris flow in the stream channel

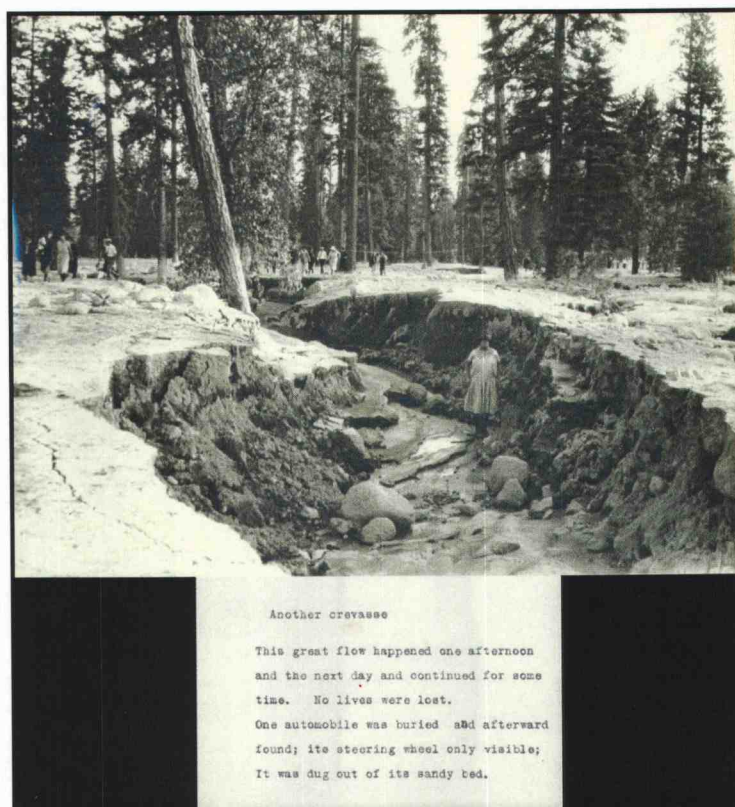


Photo 16: Depth of deposited material incised by stream flow

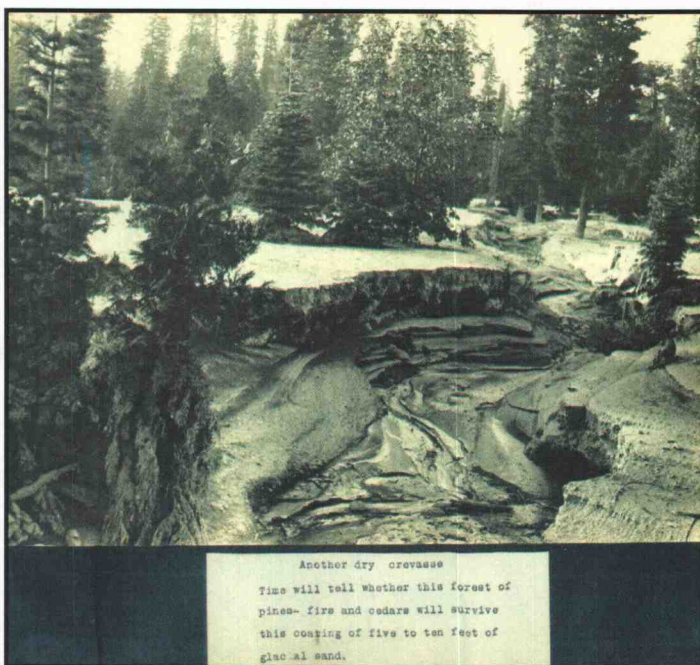


Photo 17: Mud Creek in the most heavily affected area



Photo 18: Mud Creek in the most heavily affected area

APPENDIX B**AERIAL PHOTOGRAPHY USED: WHITNEY CREEK 2003 AND MUD CREEK 1944**

The following samples of air photos used in the study of Mud and Whitney Creek lahars were obtained from the USFS McCloud Ranger District Manager's office in McCloud, California. The first set of 12 Whitney Creek 2003 air photos were scanned from prints at a scale of 1:15,840. These photos were useful in the comparison of mapped 1935 lahar deposits with the extent of the 1997 flow (Figure 6) and in a volume estimation for the 1997 lahar. The 1944 Mud Creek air photo shows the affected area 13 yr after the 1921-1931 series.

WHITNEY CREEK AND JUNIPER FLAT SERIES, 2000 AND 2001

Courtesy of Peter Van Susteren, USFS McCloud Ranger Station

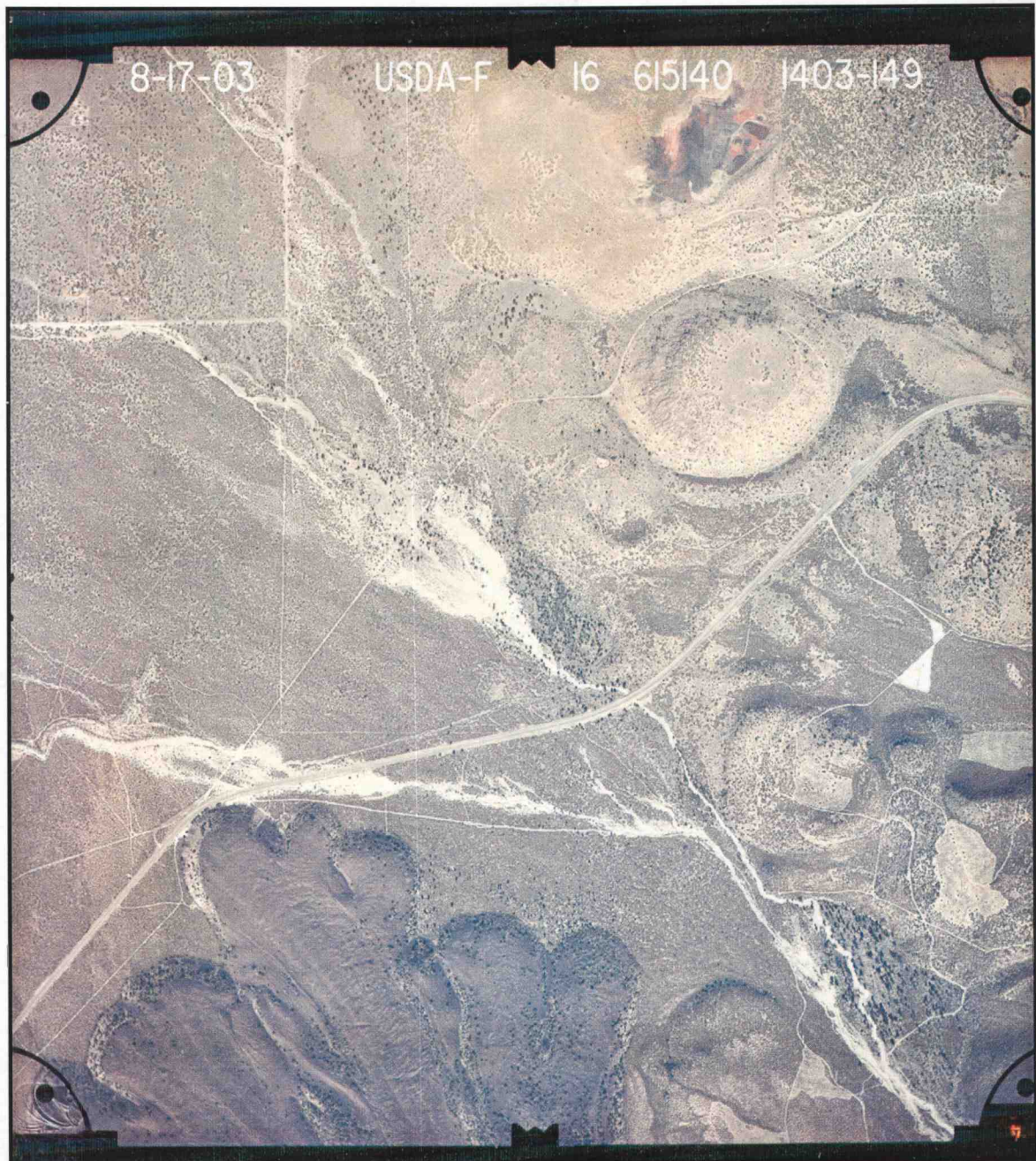


Figure B1: Whitney Creek at the intersection with U.S.97

MUD CREEK 1944 AIR PHOTO

Courtesy of Peter Van Susteren, USFS McCloud Ranger Station

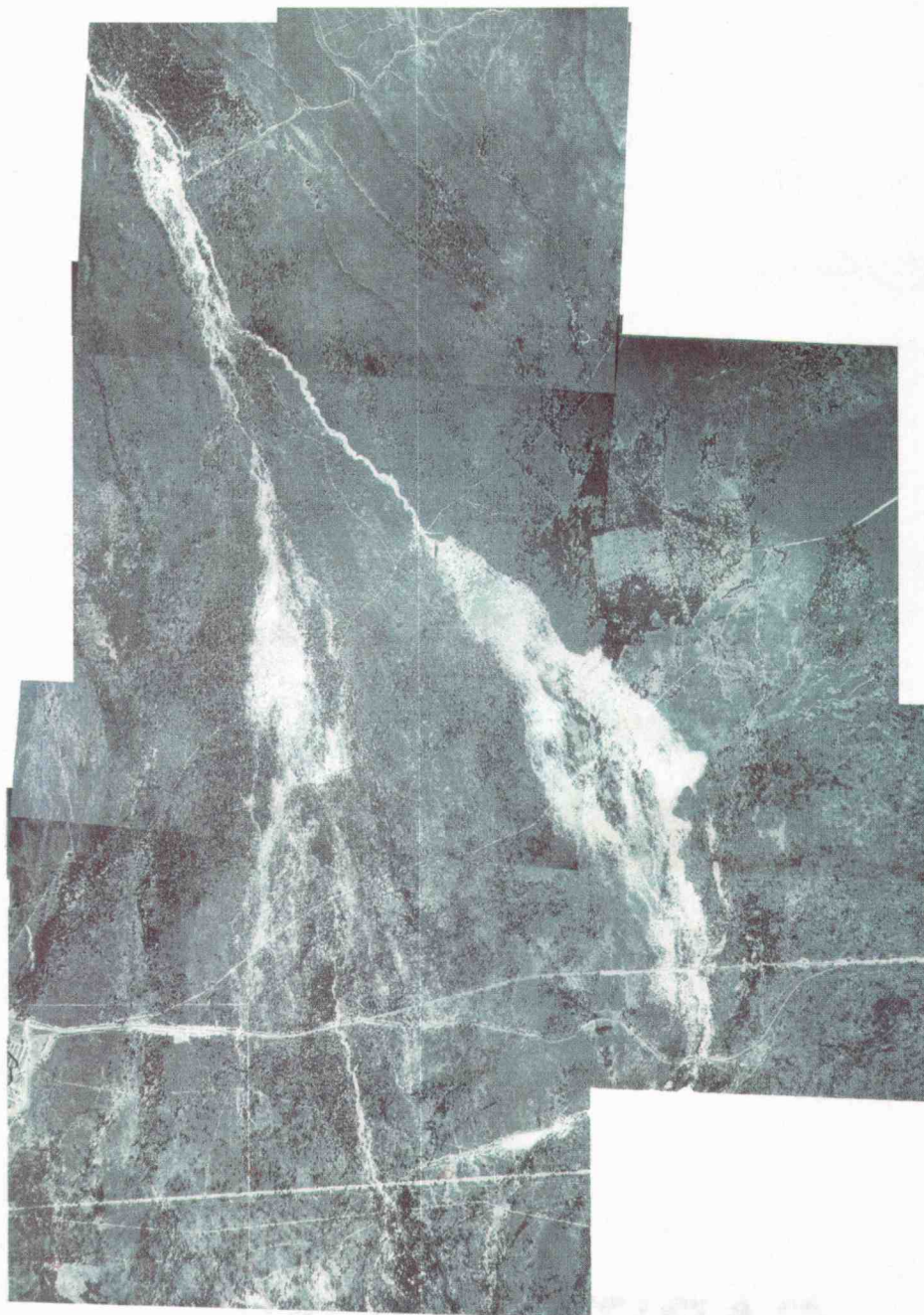


Figure B2: Entire length of the 1924-1931 Mud Creek debris flow series as it crosses Highway 89.

APPENDIX C

PREVIOUS LAHAR HAZARD MAPS OF MOUNT SHASTA, CA.

The lahar hazard zonation maps for Mount Shasta shown here were taken from work done by Miller in 1980 and Osterkamp, Hupp, and Blodgett in 1986. The map by Miller (1980) based on geological evidence of events originating from Mount Shasta during the past 10,000 yr, was an effort to raise awareness among land-use planners and other California officials of the distal extents of a range of volcanic hazards for Mount Shasta (Monmonier, 1997). This work was followed by the development of a short booklet written for the general public by Crandell and Nichols (1987) in which the destructive potential of mudflows is illustrated, along with other potential hazards from Mount Shasta. Monmonier (1997) takes the distribution of this pamphlet as an example of the complexity involved in the process of risk communication.

Local and state officials helped introduce the booklet at a public workshop, after which several thousand copies were distributed to post offices and other public venues. Officials decided not to "mass-mail" these pamphlets, as they feared it would send a false alarm, and generate unnecessary anxiety. There was also the concern that local stakeholders might consider it a threat to property values and development plans. The reaction to these hazard maps was not surprising. Someone took huge quantities of them from the public venues and they were never seen again (Monmonier, 1997).

1980 LAHAR HAZARD MAP BY D. MILLER

The 1980 lahar hazard map by D. Miller includes three hazard zones ranging from (A) areas that are most likely to be affected by lahars to (C), areas that are likely to be affected the least. As the hazard decreases everywhere within the zones with greater height above stream channels and with greater distance from Mount Shasta, no lahar hazard exists on high areas within or beyond the zones. The northeastward tendency of the high hazard zones is a reflection of the presence of glaciers on that side of the volcano.

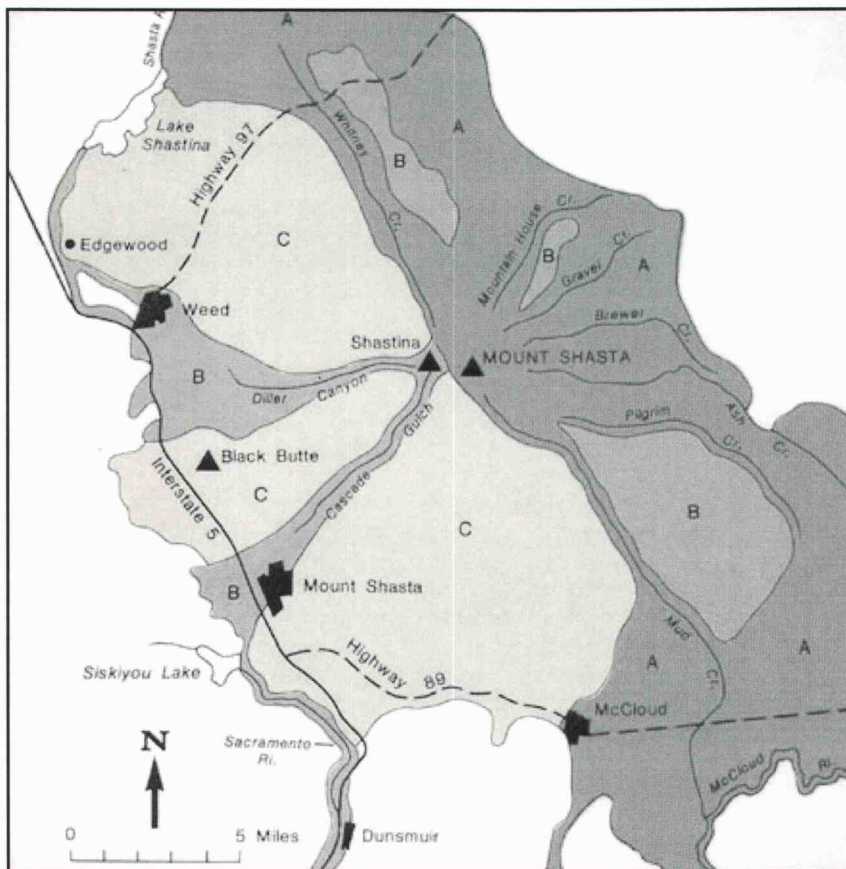


Figure C1: Mount Shasta mudflow hazard map by Miller (1980)

1986 DEBRIS FLOW HAZARD ZONES FOR WHITNEY AND MUD CREEK BY W. OSTERKAMP

Scanned from Osterkamp et al. (1986), the hazard gradations shown in shades of pink correspond to the probability that a given area will be affected by debris flow activity within the next 100 yr. The high risk areas of most frequent activity are shown in darker shades and the risk decreases progressively to lighter shades. The hazard zones are based on geological and dendrogeomorphic field evidence from Osterkamp, W. R., Hupp, C. R., and Blodgett, J. C. (1986).

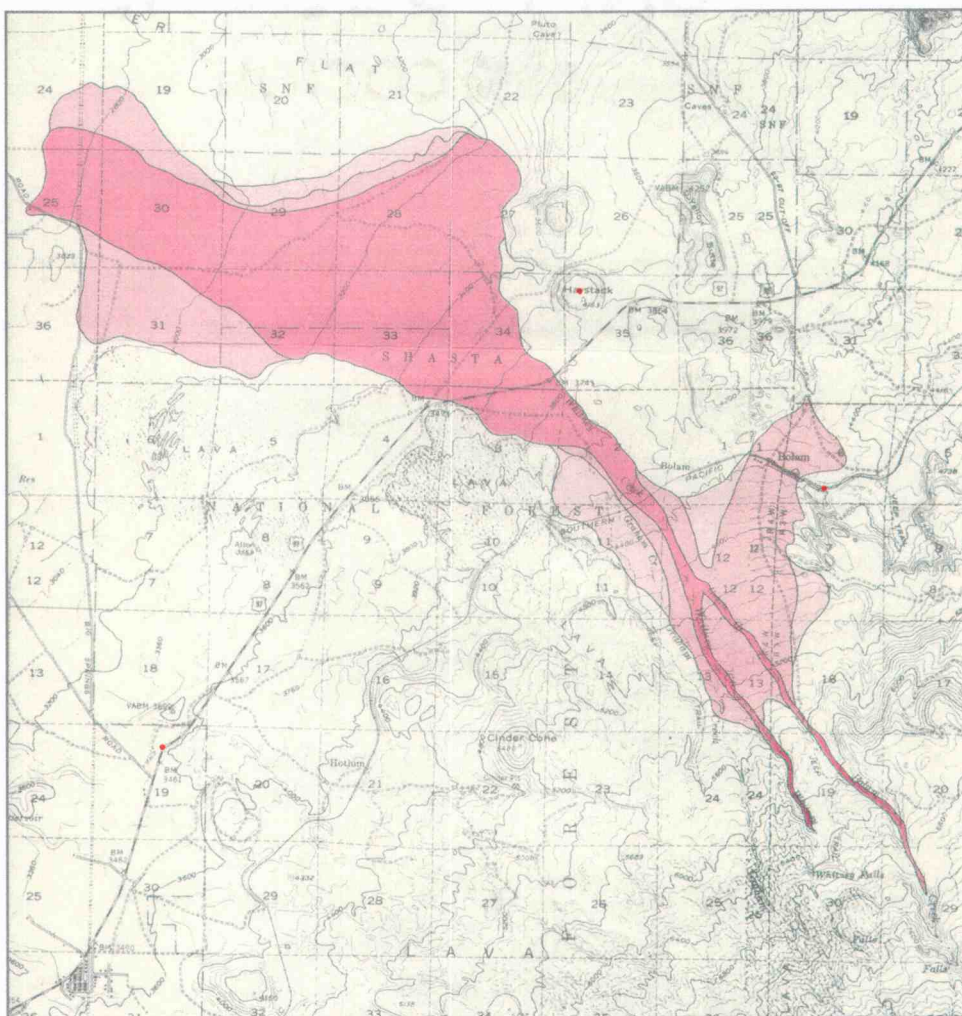


Figure C2: Scanned debris flow hazard map for the Whitney Creek drainage from Osterkamp et al. (1986)

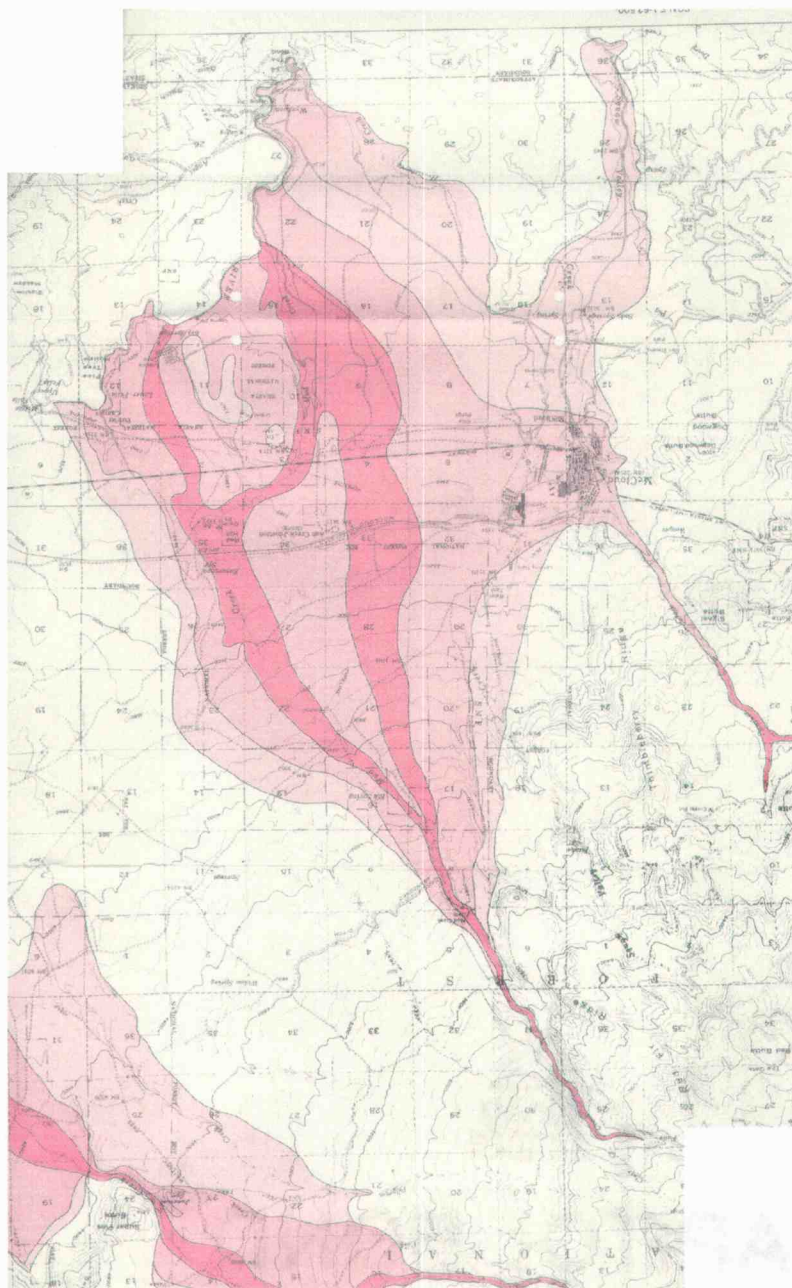


Figure C3: Scanned debris flow hazard map for the Mud Creek drainage from Osterkamp et al. (1986)

APPENDIX D

LAHARZ PROCESSING SEQUENCE AND ALGORITHM

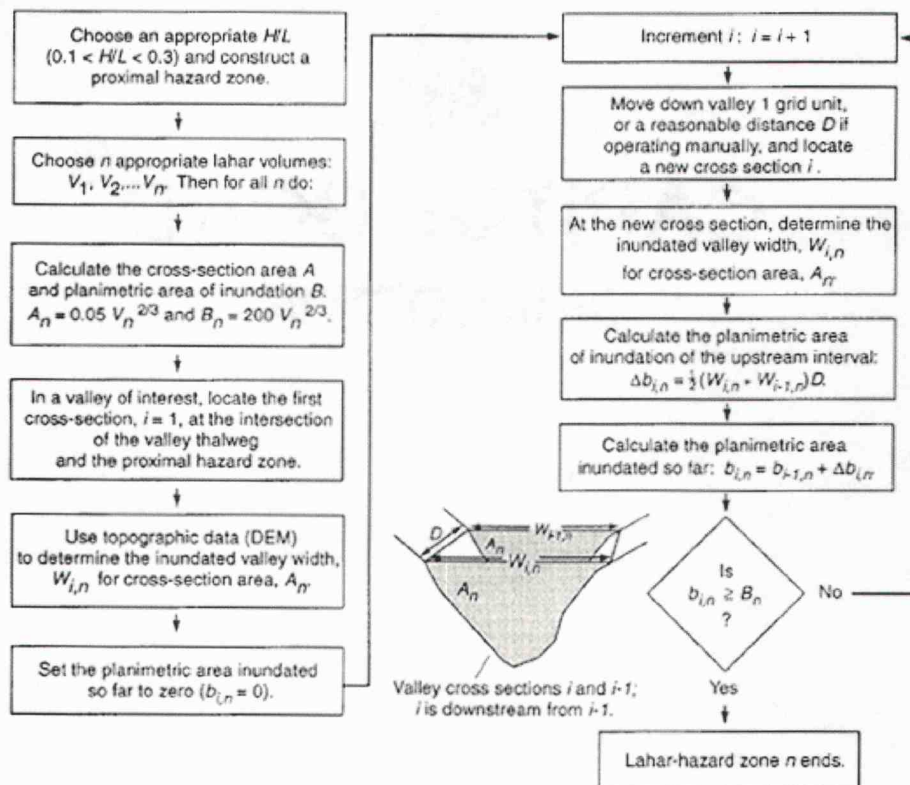


Figure D1: Flow chart of the algorithm used to implement hazard zone delineation. Modified from Iverson et al. (1998).

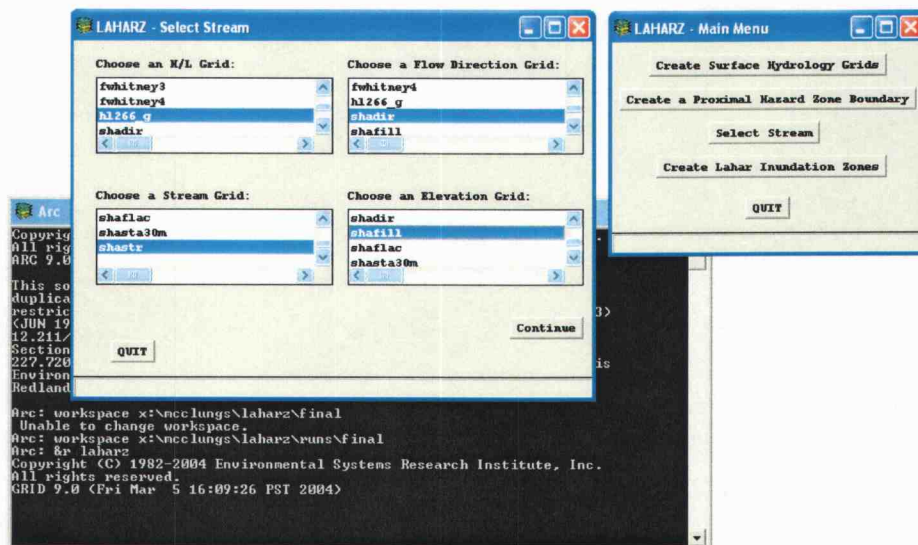


Figure D2: Screen capture of LAHARZ AML menus in action: stream selection

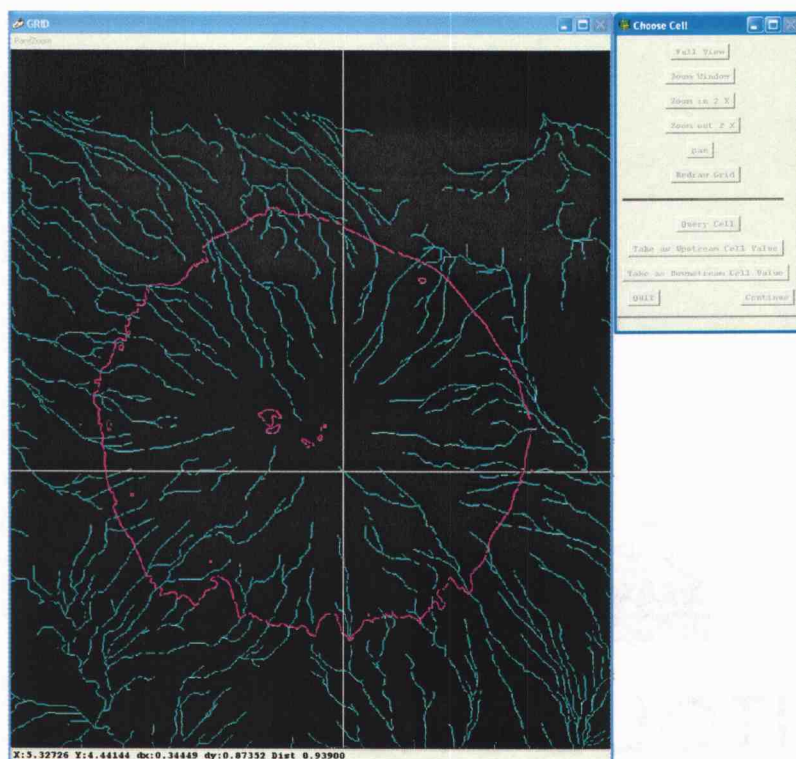
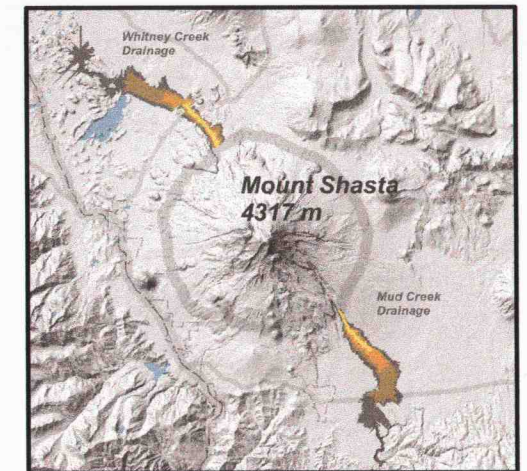
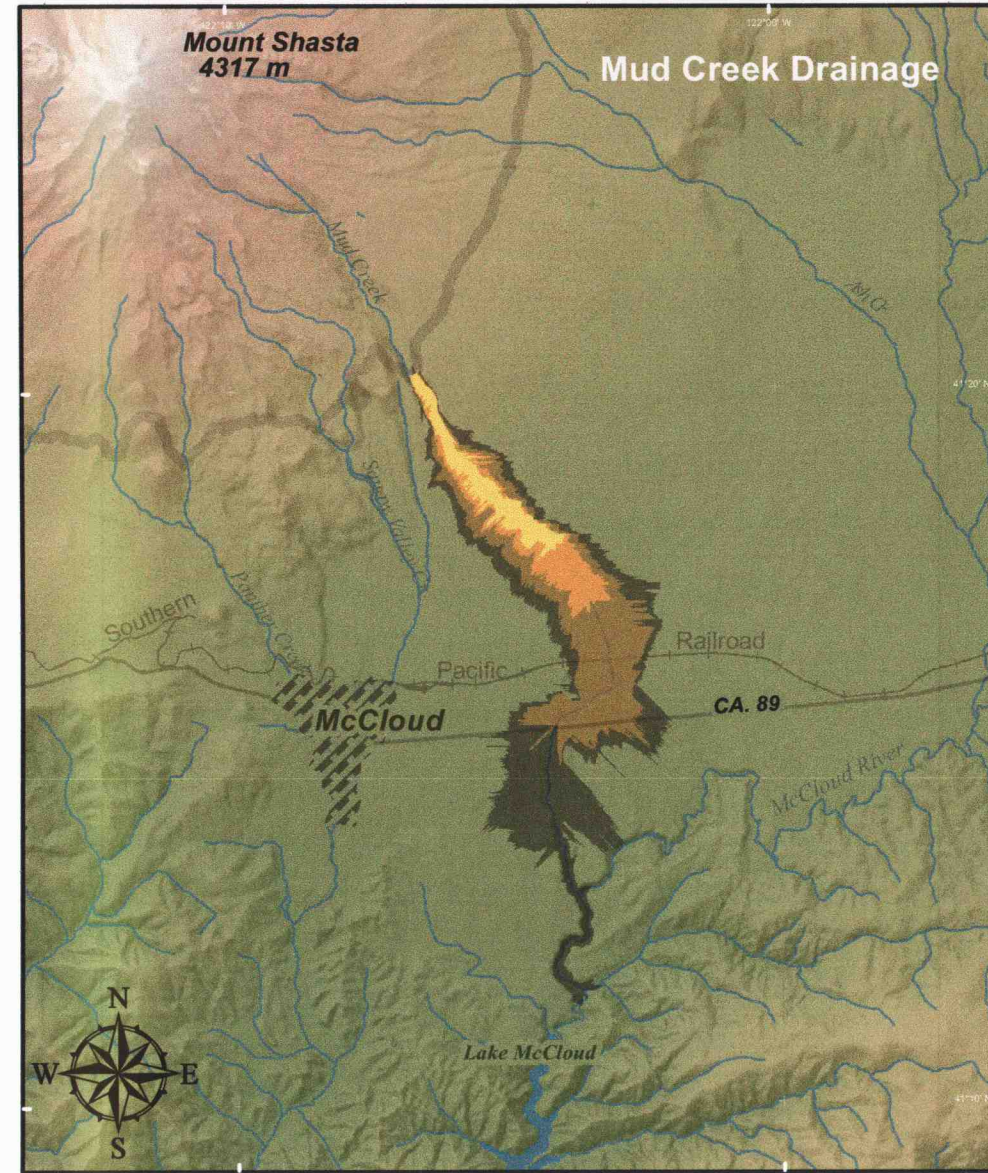
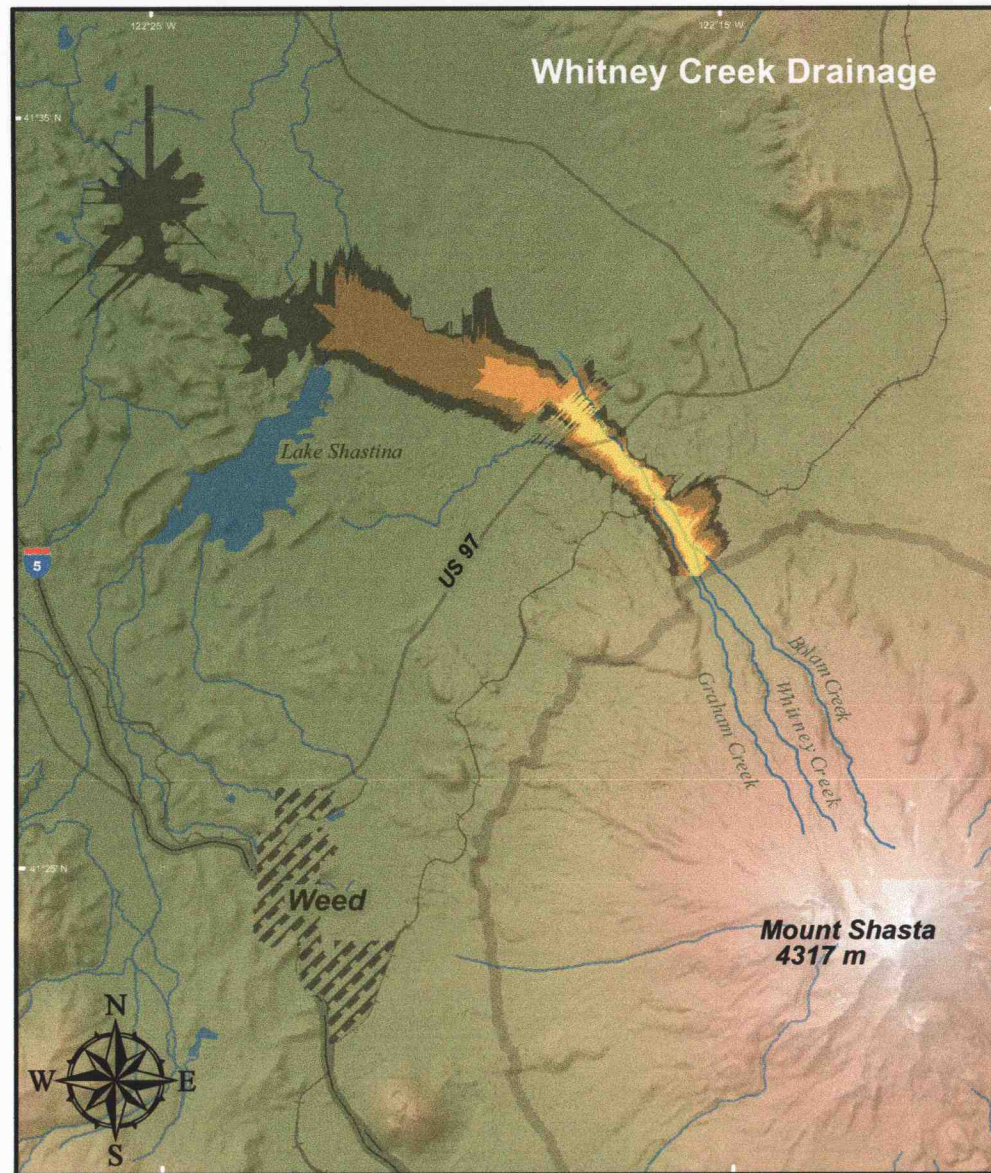


Figure D3: Screen capture of LAHARZ stream selection grid display. The crossbar is located over the initiation point for Mud Creek lahars. LAHARZ processes cell by cell downstream until it has found the proximal Hazard boundary line at which point it begins filling valley cross-sections to create inundation zones.

APPENDIX E

HAZARD ZONATION MAP FOR MUD AND WHITNEY CREEK BASINS

Lahar Inundation Hazard Zones for Mud and Whitney Creek Basins, Mount Shasta California



Proximal Hazard Zone

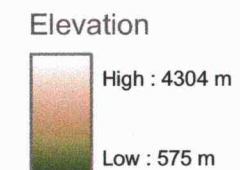
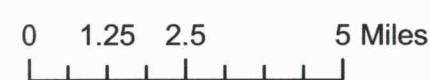
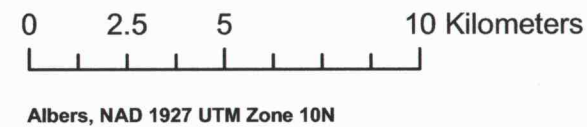
Areas that are likely to be affected most severely by pyroclastic flows, and associated ash clouds, lateral blasts, and lahars originating on Mount Shasta volcano. Debris avalanches, pyroclastic flows and lahars, which originate within the proximal hazard zone, are likely to travel further downstream beyond the flanks of the volcano and beyond the proximal hazard zone boundary.

Lahar Hazard Zones

- Areas that could be inundated by a lahar having a volume of 1,000,000 cubic meters
- Areas that could be inundated by a lahar having a volume of 5,000,000 cubic meters
- Areas that could be inundated by a lahar having a volume of 23,000,000 cubic meters
- Areas that could be inundated by a lahar having a volume of 70,000,000 cubic meters

- Main roads and highways
- Rivers and streams
- Railroads

Steve C McClung, 2005
Geosciences Department
Oregon State University



NOTE: This map contains sharp boundaries for all hazard zones. The degree of hazard does not change abruptly at these boundaries. Rather, the hazard decreases gradually as distance from the volcano increases and areas immediately adjacent to hazard zone boundaries should not be regarded as hazard free. These boundaries are located only approximately, as a degree of uncertainty exists regarding the source, size and mobility of future lahars. It should be noted, however, that hazard decreases rapidly as elevation above the valley floor increases.